AD_____

Award Number: DAMD17-02-1-0510

TITLE: A Molecular Connection between Breast Cancer Proliferation and Metastasis Mediated by Akt Kinase

PRINCIPAL INVESTIGATOR: Georg F. Weber, M.D., Ph.D.

CONTRACTING ORGANIZATION: University of Cincinnati
Cincinnati, OH 45267-0004

REPORT DATE: August 2006

TYPE OF REPORT: Final

PREPARED FOR: U.S. Army Medical Research and Materiel Command
Fort Detrick, Maryland 21702-5012

REPORT DOCUMENTATION PAGE

Form Approved
OMB No. 0704-0188

1. REPORT DATE *(DD-MM-YYYY)*	**2. REPORT TYPE**	**3. DATES COVERED** *(From - To)*
01-08-2006	Final	1 AUG 2002 - 31 JUL 2006

4. TITLE AND SUBTITLE
A Molecular Connection Between Breast Cancer Proliferation and Metastasis Mediated by Akt Kinase

5a. CONTRACT NUMBER

5b. GRANT NUMBER
DAMD17-02-1-0510

5c. PROGRAM ELEMENT NUMBER

6. AUTHOR(S)
Georg F. Weber, M.D., Ph.D.

E-Mail: georg.weber@uc.edu

5d. PROJECT NUMBER

5e. TASK NUMBER

5f. WORK UNIT NUMBER

7. PERFORMING ORGANIZATION NAME(S) AND ADDRESS(ES)
University of Cincinnati
Cincinnati, OH 45267-0004

8. PERFORMING ORGANIZATION REPORT NUMBER

9. SPONSORING / MONITORING AGENCY NAME(S) AND ADDRESS(ES)
U.S. Army Medical Research and Materiel Command
Fort Detrick, Maryland 21702-5012

10. SPONSOR/MONITOR'S ACRONYM(S)

11. SPONSOR/MONITOR'S REPORT NUMBER(S)

12. DISTRIBUTION / AVAILABILITY STATEMENT
Approved for Public Release; Distribution Unlimited

13. SUPPLEMENTARY NOTES

14. ABSTRACT:

Death from cancer is most frequently caused by metastases. While research of the past 25 years has identified genes whose malfunction causes cancer to grow, it has not been clear why these defects also induce the ability to metastasize. We have defined molecules that form a connection between signals that make cancer cells grow and signals that cause them to metastasize. In breast cancer cells, a molecule called Akt kinase bridges these two functions. Here we study the exact mechanism by which Akt kinase connects mechanisms of growth with mechanisms of cancer spread. The identification of a single defined defect as responsible for growth and metastasis enhances our molecular insights into cancer and it defines candidate targets for therapeutic intervention.

15. SUBJECT TERMS
Cell signaling, metastasis, growth dysregulation, Akt kinase

16. SECURITY CLASSIFICATION OF:			**17. LIMITATION OF ABSTRACT**	**18. NUMBER OF PAGES**	**19a. NAME OF RESPONSIBLE PERSON**
a. REPORT	**b. ABSTRACT**	**c. THIS PAGE**			USAMRMC
U	U	U	UU	43	**19b. TELEPHONE NUMBER** *(include area code)*

Table of Contents

Summary

We had proposed to study the roles of osteopontin as a metastasis gene and downstream target of Akt kinase in breast cancer. The basic observations defining these molecular connections were published in 2003 [Zhang et al. Molecular and Cellular Biology]. Our research plan included six tasks, of which 1, 2, 4, 5, and 6 have been completed successfully. Although task 3 was not accomplished, we have made progress beyond the original proposal. We observed that osteopontin is often spliced in human cancer cells. We expanded our studies within task 5 to include all the variant forms of osteopontin. This has resulted in a 2006 publication in a high impact cancer journal [He et al. Oncogene]. We believe that our work has provided important new insights into the expression and function of osteopontin in breast cancer. We hope that these findings will lead to diagnostic and therapeutic applications. Without the support form the USAMRMC this work would not have been possible.

Introduction

The defining characteristics of benign and malignant tumors are excessive growth and immortalization. In contrast, only malignant tumors express gene products that mediate invasiveness. Uncontrolled proliferation is a consequence of gain-of-function mutations of proto-oncogenes or loss-of-function mutations of tumor suppressor genes. Metastatic dissemination is a consequence of aberrant expression or splicing of stress response genes [Weber/Ashkar 2000]. The consistent topology of metastasis formation by specific cancers, such as the high frequency of colony formation in bone and brain by malignant breast tumors, implies that metastasis gene expression is an inevitable consequence of gain of function by specific oncogenes. This raises the question: What molecular mechanisms connect the signal transduction pathways associated with dysregulated growth to the expression of metastasis genes in malignant, but not in benign tumors?

Receptor ligation by the epidermal growth factor EGF can induce osteopontin gene expression [Malyankar et al. 1997; Atkins et al. 1997] through signal transduction that proceeds via protein kinase C and tyrosine kinases [Chackalaparampil et al. 1996].

This implies that gain-of-function mutations in the EGF receptor pathway in breast cancer, causing dysregulated growth, may also mediate the over-expression of osteopontin, leading to dissemination. We find osteopontin to be constitutively expressed in malignant, but not in benign transformed breast cells. We have mapped the cause for this to the constitutive activation of Akt kinase, an enzyme that is part of the EGF signaling pathway [Zhang et al. 2003].

SOW

Specific Aim 1: Molecular characterization of the role of AKT in proliferation and induction of metastasis genes

Task 1: Transfection ofAkt, dnAkt, constitutively active Akt, or vector control into breast epithelial cells. Cloning and characterization of the transfectants. Deliverable: Stably transfected cell lines. 3 months.

Task 2: Analysis of the changes in osteopontin expression, expression of cyclins, and changes in cell cycle profile after transfection of Akt kinase, constitutively active Akt kinase, or dominant negative Akt kinase. Deliverable: Definition of the role of Akt in proliferation and osteopontin expression on the genetic level. 6 month.

Specific Aim 2: Identification of downstream targets of Akt in osteopontin induction and cell cycle progression.

Task 3: Analysis of changes in proliferative and anti-apoptotic signaling molecules that act downstream of Akt. Deliverable: Data on changes in p27kip, Bad, caspase-9, and FKHR after transfection with Akt or its variants in the presence or absence of EGF. 7 months.

Task 4: Cloning of the osteopontin promoter into a reporter construct and investigation into reporter activity in various transfectants of Akt, constitutively active Akt, or dominant negative Akt. Electrophoretic mobility shift assays of nuclear extracts from the transfectants with oligonucleotides derived from the osteopontin promoter. Deliverable: Identification of Akt-induced transcription factors that mediate osteopontin gene expression. 5 months.

Specific Aim 3: Analysis of metastatic potential dependent on Akt and osteopontin

Task 5: Study of colony formation of transfected cells (vector, Akt, constitutively active Akt, dominant negative Akt) in soft agar in the presence or absence of anti-OPN antibody or after co- transfection with osteopontin antisense. Deliverable: Data on dependence of growth in soft agar on Akt and osteopontin. 3 months.

Task 6: In vivo analysis of dissemination of cells transfected with Akt, constitutively active Akt, dominant negative Akt, vector control after orthotopic injection. Deliverable: Data on dependence of metastasis formation on Akt and osteopontin. 9 months. This task will use a maximum of 100 mice.

Body

Specific Aim 1: Molecular characterization of the role of AKT in proliferation and induction of metastasis genes

Task 1: Transfection of Akt, dnAkt, constitutively active Akt, or vector control into breast epithelial cells. Cloning and characterization of the transfectants. Deliverable: Stably transfected cell lines. 3 months.

We stably transduced murine breast epithelial cells with various Akt kinase constructs. Benign cells were transfected with vector, wild-type Akt, or constitutively active Akt, while malignant cells were transfected with vector, wild-type Akt, or a dominant negative Akt mutant. The expression levels of the transfected genes were measured on the RNA and protein levels. Expectedly, osteopontin was constitutively expressed in Akt kinase-transduced cells and the constitutive osteopontin gene expression in malignant cells was suppressed by the dominant negative Akt kinase mutant according to RNAse protection assay, Northern blotting, and Western blotting. The levels of osteopontin induced by wild-type Akt and constitutively active Akt are comparable, likely reflecting the substantial overexpression. At these amounts, the baseline activity of wild-type Akt kinase is sufficient to transduce a signal. It may be important to note that the reduction of osteopontin gene expression by dominant negative Akt kinase is partial. Only moderate levels of over-expression can be achieved for dominant negative Akt kinase because this mutant also slows down cell divisions, consistent with the hypothesis that the constitutive activation of Akt kinase in aggressive breast cancer cells is causative for the transformation of these cells [Zhang et al. 2003].

Task 2: Analysis of the changes in osteopontin expression, expression of cyclins, and changes in cell cycle profile after transfection of Akt kinase, constitutively active Akt kinase, or dominant negative Akt kinase. Deliverable: Definition of the role of Akt in proliferation and osteopontin expression on the genetic level. 6 month.

In order to differentiate between osteopontin-dependent and osteopontin-independent consequences of Akt kinase overexpression we generated doubly transduced

lines. Benign cells (Comma-D, FSK-7) that stably expressed constitutively active Akt kinase were infected with a retrovirus containing osteopontin antisense. Similarly, we generated malignant (MT2994) dominant negative Akt/osteopontin cells. All relevant singly and doubly transfected controls were included. As before, the expression levels of the modulated genes were measured by Western blotting. The elevated osteopontin expression in transfectants of constitutively active Akt kinase could be reversed by co-transfection of antisense osteopontin, and the suppression of osteopontin by dominant negative Akt was reversed by co-transfection with the osteopontin gene. We tested the growth rates of doubly transduced cells by plating 5000 cells per well in 24-well plates followed by daily cell counts in quintuplicates. Remarkably, within only one day, transfection of constitutively active Akt kinase into benign cells significantly induced the growth rate, while transfection of dominant negative Akt kinase into malignant cells significantly reduced it. The differences remained significant throughout the four days of measurement. In contrast, the stable transfection of osteopontin into cells overexpressing dominant negative Akt kinase or of osteopontin antisense into cells overexpressing constitutively active Akt kinase had no effect on the growth rates. We also analyzed cell motility by in vitro wounding and transwell chemokinesis. Benign cells transfected with constitutively active Akt displayed enhanced migration. Co-transfected osteopontin antisense completely reversed this effect [Zhang et al. 2003]. These results are consistent with osteopontin-independent roles of Akt as a growth promoting gene product and osteopontin-dependent roles of Akt as a migration promoting gene product.

Specific Aim 2: Identification of downstream targets of Akt in osteopontin induction and cell cycle progression.

Task 4: Cloning of the osteopontin promoter into a reporter construct and investigation into reporter activity in various transfectants of Akt, constitutively active Akt, or dominant negative Akt. Electrophoretic mobility shift assays of nuclear extracts from the transfectants with oligonucleotides derived from the osteopontin promoter. Deliverable: Identification of Akt-induced transcription factors that mediate osteopontin gene expression. 8 months.

Previous studies have shown that the induction of osteopontin in renal epithelial cells by TGF-β or EGF is caused by increased transcription [Malyankar et al. 1997]. Akt kinase activity has previously been associated with activation of the AP-1 transcription factor and Ets-family transcription factors, both of which are known to bind to the osteopontin promoter. We set out to further map the molecular connections between Akt kinase activity and osteopontin transcription in breast epithelial cells. For this purpose, we took advantage of the breast epithelial cell lines constitutively expressing various Akt constructs that we had generated. We used benign cells stably expressing wild-type Akt kinase, constitutively active Akt kinase, or vector in luciferase reporter assays under the control of full length or truncated osteopontin promoter sequences. Expectedly, Akt kinase activity can induce the transactivation of the osteopontin promoter [Zhang et al. 2003]. The Akt responsive promoter domain was mapped to a region between base –600 and base –777. Consistent with a previous report [Guo et al. 1995], a far distal promoter element (between bases –777 and -882) appeared to contain a repressor element.

Specific Aim 3: Analysis of metastatic potential dependent on Akt and osteopontin

Task 5: Study of colony formation of transfected cells (vector, Akt, constitutively active Akt, dominant negative Akt) in soft agar in the presence or absence of anti-OPN antibody or after co- transfection with osteopontin antisense. Deliverable: Data on dependence of growth in soft agar on Akt and osteopontin.

Because osteopontin is necessary for soft agar colony formation and Akt kinase induces osteopontin expression we asked whether the constitutive over-expression of Akt kinase in benign cells was sufficient to convey the ability of anchorage independent growth. Expectedly, Akt transfected breast epithelial cells displayed clone formation in soft agar, whereas vector transfected cells did not. The repeated addition of an anti-osteopontin antibody to the cell culture reduced the numbers and sizes of clones formed. In contrast, a control immunoglobulin had no effect [Zhang et al. 2003]. We also analyzed the doubly transduced cells for colony formation in soft agar. Co-expression of osteopontin antisense in constitutively active Akt expressing cells lead to a partial reduction of colony formation, while cells transduced with vector constructs did not form

clones in soft agar. In a complementary approach, the expression of dominant negative Akt in malignant cells caused a partial reduction in the numbers and sizes of clones formed. Co-expression of osteopontin virtually completely reversed this inhibition [Zhang et al. 2003].

We analyzed osteopontin gene expression in various breast tumor cells by RT-PCR. To eliminate skewing of the results by activation of the cells through growth factors in the medium, we used serum-free conditions. The malignant breast cancer cell lines MDA-MB-435 and MDA-MB-231 express three distinct RNA messages of osteopotin. MCF-7 cells are non-invasive and do not contain measurable osteopontin RNA levels. Other invasive cell lines tested, including cancers of diverse tissue origin, express multiple osteopontin messages (Hela, SAOS-2, 21MT1, 21MT2), while all non-invasive cell lines tested (ZR-75-1, 21NT, LnCAP) express no osteopontin or low levels of osteopontin-a without splice variants. The secretion of multiple osteopontin forms by the invasive breast cancer cell line MDA-MB-435, but not by the non-invasive breast tumors MCF-7 and ZR-75-1 was confirmed by Western blotting [He et al. 2006]. The two smaller osteopontin transcript bands selectively expressed in malignant cells were identified by cloning and sequencing as splice variants missing the third or fourth translated exons (exons 4 or 5, because exon 1 is untranslated [Behrend et al. 1993]). The identified transcripts correspond to the sequences of “osteopontin-a”, “osteopontin-b”, and “osteopontin-c”, which are listed in GenBank (Accession numbers D28759, D28760, and D28761) but have not been thoroughly studied. Published reports on the expression or function of the splice variants are limited to the observation of three types of osteopontin RNA messages in human gliomas [Saitoh et al. 1995] and to the existence of a splice variant that has a deletion in its N-terminal portion [Kiefer et al. 1989].

We stably transduced full length osteopontin (variant a) and splice variant c into MCF-7 cells, which do not express endogenous osteopontin. Because we had previously found osteopontin to facilitate clone formation in soft agar [Zhang et al. 2003], we tested whether the transfection of osteopontin-a or osteopontin-c changed the phenotype of MCF-7 cells in this assay. In fact, osteopontin-c facilitated soft agar clone formation and

the clones formed after 7 days show distinct protrusions, which are absent from osteopontin-a transfected cells or vector controls and which we believe to be indicative of the rapid expansion of the clones within the agar [He et al. 2006]. These changes were directly dependent on the osteopontin protein because the addition of anti-osteopontin antibody, but not control immunoglobulin, to the cultures every other day with the exchange of medium suppressed the formation of clones by the transfected MCF-7 cells. In contrast, the antibody had no effect on the clones formed by vector transfected MCF-7 cells. The clone sizes of osteopontin-a transfected MCF-7 cells were moderately, but statistically significantly, larger than the vector control, and osteopontin-c transfected cells formed significantly larger colonies than osteopontin-a transfectants [He et al. 2006].

To account for the changes in soft agar growth characteristics, we first asked whether the growth rates of the osteopontin expressing MCF-7 transfectants were altered as compared to a vector transfected MCF-7 clone. Consistent with our earlier results, which had indicated that osteopontin expression affects motility but not cell growth [Zhang et al. 2003], there were no differences in cell numbers among MCF-7-vector, MCF-7-osteopontin-a, and MCF-7-osteopontin-c over 6 days of analysis. Because different growth rates did not account for the distinct phenotypes generated by osteopontin-a and osteopontin-c in soft agar, we set out to analyze MCF-7 cell adhesion as a factor that regulates anchorage-independence. We found that osteopontin-a, but not osteopontin-c, had a tendency to aggregate in the presence of physiologic concentrations of calcium. Chelation with EDTA could prevent this phenomenon and magnesium, another divalent cation, could not substitute for calcium. The phenomenon observed in serum-free supernatants from transfected cells could be reproduced with purified GST-OPN. MCF-7 cells adhered to and spread on supernatants from osteopontin transfected cells and on dose-dependently increasing amounts of purified recombinant GST-OPN. When plated with increasing amounts of calcium, the adhesion to osteopontin-a, but not to osteopontin-b or osteopontin-c, became stronger [He et al. 2006].

To further characterize the molecular basis for the enhancement of soft agar colony formation by osteopontin-c, we extracted the cellular RNA after 7 days of growth in soft agar and performed microarray analysis comparing MCF-7 OPNc to MCF-7 OPNa or to MCF-7 vector. The groups of genes affected by osteopontin-c (as compared to vector) include oxidoreductases and ion transporters according to EASE (Expression Analysis Systematic Explorer) analysis [He et al. 2006].

Task 6: In vivo analysis of dissemination of cells transfected with Akt, constitutively active Akt, dominant negative Akt, vector control after orthotopic injection. Deliverable: Data on dependence of metastasis formation on Akt and osteopontin. 9 months. This task will use a maximum of 100 mice.

We tested in vivo tumorigenesis and dissemination by the doubly transduced benign cells. Expectedly, the vector/vector and vector/antisense osteopontin transduced cells generated small hyperplastic lesions. In contrast, caAkt expressing cells generated larger tumors. Only the cells containing Akt plus vector, but not the cells expressing Akt plus antisense osteopontin, formed distal lesions [Zhang et al. 2003].

Note

At the turn of the year 2003/2004, this laboratory moved from the New England Medical Center, Boston, to the University of Cincinnati. The transfer of the grant was delayed, mostly because of slow relinquishing from the New England Medical Center. Therefore, a one-year no-cost extension was granted.

Key Research Accomplishments

* We have identified the constitutive activation of Akt kinase as a molecular defect in malignant breast cancer.

* Our laboratory and others have shown that osteopontin gene expression is essential for generating a malignant phenotype in breast tumors.

* We have found osteopontin gene expression to be a downstream target of Akt activity.

* We can differentiate two signal transduction cascades downstream of Akt that lead to either growth dysregulation or invasiveness.

* We found that not only osteopontin expression but also osteopontin splicing is a determining factor for breast cancer malignancy.

* Invention disclosures for these observations have been submitted to the University Office for Technology Transfer and the University of Cincinnati Intellectual Property Office.

Reportable Outcomes

Zhang G, He B, **Weber GF**. 2003. Growth factor signaling induces metastasis genes in transformed cells. A molecular connection between Akt kinase and osteopontin in breast cancer. Molecular and Cellular Biology 23:6507-6519.

He B, Mirza M, **Weber GF**. 2006. An osteopontin splice variant induces anchorage independence in human breast cancer. Oncogene 25:2192-2202.

Zhang G, He B, **Weber GF**. A molecular connection between oncogenes and metastasis genes in malignant breast cancer. Era of Hope (DOD Breast Cancer Research Program). Philadelphia June 2005.

Conclusions

Like other aspects of cancer, metastasis is caused by the dysregylation of specific genes.

Metastasis genes are stress response genes, which suggests that malignancy constitutes mimicry of leukocyte homing.

In cancer, metastasis genes are aberrantly expressed or spliced.

The dysregulation of metastasis genes in cancer occurs secondary to oncogene activation.

References

Atkins KB, Simpson RU, Somerman MJ. 1997. Stimulation of osteopontin mRNA expression in HL-60 cells is independent of differentiation, *Arch Biochem Biophys* 343:157-163.

Behrend EI, Chambers AF, Wilson SM, Denhardt DT. Comparative analysis of two alternative first exons reported for the mouse osteopontin gene. J Biol Chem 1993;268:11172-5.

Chackalaparampil I, Peri A, Nemir M, Mckee MD, Lin PH, Mukherjee BB, Mukherjee AB. 1996. Cells in vivo and in vitro from osteopetrotic mice homozygous for c-src disruption show suppression of synthesis of osteopontin, a multifunctional extracellular matrix protein. *Oncogene* 12:1457-1467.

Guo X, Zhang YP, Mitchell DA, Denhardt DT, Chambers AF. 1995. Identification of a ras-activated enhancer in the mouse osteopontin promoter and its interaction with a putative ETS-related transcription factor whose activity correlates with the metastatic potential of the cell. *Mol Cell Biol* 15:476-487.

He B, Mirza M, Weber GF. 2006. An osteopontin splice variant induces anchorage independence in human breast cancer. Oncogene 25:2192-2202.

Kiefer MC, Bauer DM, Barr PJ. The cDNA and derived amino acid sequence for human osteopontin. Nucl Acids Res 1989;17:3306.

Malyankar UM, Almeida M, Johnson RJ, Pichler RH, Giachelli CM. 1997. Osteopontin regulation in cultured rat renal epithelial cells. *Kidney Int* 51:1766-1773.

Saitoh Y, Kuratsu J, Takeshima H, Yamamoto S, Ushio Y. Expression of osteopontin in human glioma. Its correlation with the malignancy. Lab Invest 1995;72:55-63.

Weber GF, Ashkar S. 2000. Stress response genes - the genes that make cancer metastasize. *J Mol Med* 78:404-408.

Zhang G, He B, Weber GF. 2003. Growth factor signaling induces metastasis genes in transformed cells. A molecular connection between Akt kinase and osteopontin in breast cancer. *Mol Cell Biol* 23:6507-6519.

Appendix

Zhang G, He B, **Weber GF**. 2003. Growth factor signaling induces metastasis genes in transformed cells. A molecular connection between Akt kinase and osteopontin in breast cancer. Molecular and Cellular Biology 23:6507-6519.

He B, Mirza M, **Weber GF**. 2006. An osteopontin splice variant induces anchorage independence in human breast cancer. Oncogene 25:2192-2202.

MOLECULAR AND CELLULAR BIOLOGY, Sept. 2003, p. 6507–6519 Vol. 23, No. 18
0270-7306/03/$08.00+0 DOI: 10.1128/MCB.23.18.6507–6519.2003

Growth Factor Signaling Induces Metastasis Genes in Transformed Cells: Molecular Connection between Akt Kinase and Osteopontin in Breast Cancer

Guoxin Zhang,[1]† Bin He,[1] and Georg F. Weber[1,2]*

Department of Radiation Oncology, New England Medical Center,[1] and Sackler School of Graduate Biomedical Sciences, Tufts University School of Medicine,[2] Boston, Massachusetts

Received 10 December 2002/Returned for modification 20 February 2003/Accepted 19 June 2003

Malignant tumors are characterized by excessive growth, immortalization, and metastatic spread, whereas benign tumors do not express gene products that mediate invasion. The molecular basis for this difference is incompletely understood. We have screened signal transduction molecules associated with the epidermal growth factor (EGF) receptor and have identified constitutive phosphorylation, indicative of activation, of Akt kinase in MT2994 breast cancer cells. In contrast, cells of the benign breast epithelial cell lines Comma-D and FSK-7 are immortalized through pathways that are independent of the EGF–phosphatidylinositol 3-kinase–Akt kinase cascade, but this is not associated with invasiveness. Transfection of constitutively active Akt kinase causes accelerated cell division and osteopontin expression. Conversely, dominant-negative Akt kinase slows cell cycle progression and suppresses osteopontin expression. The manipulation of osteopontin expression in this setting by transfection of the gene or its antisense does not affect the growth rate of the cells but alters cell motility and anchorage independence. Therefore, Akt kinase activates two distinct genetic programs: the program of growth and survival, which is independent of osteopontin expression, and the program of invasiveness and anchorage independence, which is mediated by osteopontin. These studies define Akt kinase as a molecular bridge between cell cycle progression and dissemination.

The defining characteristics of benign and malignant tumors are excessive growth and immortalization. In contrast, only malignant tumors express gene products that mediate invasiveness. Uncontrolled proliferation is a consequence of gain-of-function mutations of proto-oncogenes or loss-of-function mutations of tumor suppressor genes. Metastatic dissemination is a consequence of aberrant expression or splicing of stress response genes (53). The consistent topology of metastasis formation by specific cancers, such as the high frequency of colony formation in bone and brain by malignant breast tumors, implies that metastasis gene expression is an inevitable consequence of gain of function by specific oncogenes. This raises the following question: what molecular mechanisms connect the signal transduction pathways associated with dysregulated growth to the expression of metastasis genes in malignant but not in benign tumors?

Gain-of-function mutations in the epidermal growth factor (EGF) family of receptors and their associated pathways of signal transduction often underlie the transformation of breast tissue, as is evidenced by the cases of breast cancers that overexpress the EGF family receptor Her-2/neu. This dysregulation is also prominent in steroid hormone-independent breast cancer, where excessive activation of EGF receptor pathways may be the only driving force for cell cycle progression (5). The intracellular signal transduction associated with members of the EGF receptor family is mediated by multiple proto-oncogene products, including protein kinase C, phosphatidylinositol 3-kinase (PI 3-kinase), and Akt kinase (31, 35). Their constitutive activation occurs as a consequence of overexpression of Her-2/neu (6, 24, 33, 41, 56) and may be sufficient to cause transformation.

Expression of the cytokine osteopontin is necessary and may be sufficient for the formation of metastases by breast cancer. High levels of osteopontin in the disease are an adverse prognostic factor (42, 45). Multiple metastatic breast cancer cell lines express osteopontin, and transfection of the osteopontin gene into weakly tumorigenic human breast tumor cell lines confers invasive behavior (47, 50, 51). Increasing the expression of osteopontin or transfection of osteopontin-encoding cDNA into a previously benign cell line is sufficient to produce a metastatic phenotype in a rat mammary model (38). Short regulatory DNAs exist in human cancer cells that can be transferred into model rat mammary cell lines and can induce metastatic spread. These noncoding fragments of DNA act via the common effector gene osteopontin (4, 11, 19, 20).

Receptor ligation by EGF can induce osteopontin gene expression (2, 34) through signal transduction that proceeds via protein kinase C and tyrosine kinases (8). This implies that gain-of-function mutations in the EGF receptor pathway in breast cancer, causing dysregulated growth, may also mediate the overexpression of osteopontin, leading to dissemination. We find osteopontin to be constitutively expressed in malignant but not in benign transformed breast cells. Here, we trace the cause for this to constitutive activation of Akt kinase, an enzyme that is part of the EGF signaling pathway.

* Corresponding author. Mailing address: Department of Radiation Oncology, New England Medical Center and Tufts University Medical School, 750 Washington St., NEMC #824, Boston, MA 02111. Phone: (617) 636-9013. Fax: (617) 636-1766. E-mail: gweber@tufts-nemc.org.

† Present address: Department of Gastroenterology, First Affiliated Hospital of Nanjing Medical University, Nanjing 210029, People's Republic of China.

MATERIALS AND METHODS

Cells. We used three murine BALB/c breast tumor cell lines with various levels of malignancy (3, 26, 29, 39). Comma-D cells are derived from culture of mid-pregnancy mammary glands and develop hyperplasia when injected into mice. FSK-7 cells were obtained from primary breast cell culture. MT2994 cells were selected from mammary tumors that had been induced by dimethylbenz[*a*]anthracene. Among these cells, only MT2994 is malignant in vivo. Even though these cell lines were derived from various mice at various time points, their shared inbred genomic background (the BALB/c strain) allows them to be viewed as a progression series of breast tumor cell lines. The cells were grown in MECL medium (Dulbecco's modified Eagle medium–Ham F-12 medium [1:1] with 2% adult bovine serum, 5 ng of EGF/ml, and 10 μg of insulin/ml). For growth factor deprivation, the medium was made without serum, EGF, and insulin.

Induction of growth factor signaling. Cells were plated at 5×10^5 per well in 6-well plates. After 7 h, cultures were washed twice with phosphate-buffered saline and maintained in growth factor-deprived medium (containing 0.05% bovine serum albumin) for 14 h. The cells were then stimulated with the indicated amounts of EGF (obtained from Sigma, St. Louis, Mo.) for the indicated time frames before harvesting and analysis.

To assess candidate signal transduction molecules involved in the induction of osteopontin gene expression, specific inhibitors were added to the cells. The PI 3-kinase inhibitor wortmannin and the phospholipase C (PLC) inhibitor U73122 were purchased from Calbiochem (San Diego, Calif.). The cells were pretreated with the respective inhibitors or vehicle (dimethyl sulfoxide) alone for 30 min and then cotreated with EGF for an additional 8 h. Preliminary dose-response experiments had established that the concentrations of 100 nM wortmannin and 500 nM U73122 were effective and nontoxic.

For the investigation of cell growth rates, each cell line was plated at 5,000 cells/well in 24-well plates. Daily, five wells per group were harvested by trypsinization, and the cell numbers were determined in a Coulter Z-Series Counter. At each time point, the cell numbers from the five wells of the various groups of transfectants were analyzed for statistically significant differences by the Wilcoxon-Mann-Whitney test, by accepting a probability of error of $<5\%$. The cell viability was always higher than 95%.

RNase protection assay. Osteopontin expression was analyzed by an RNase protection assay on total RNA by using a 400-bp probe from the 3′ region of the transcript and controlling for loading with a probe for β-actin. Total RNA was isolated using the RNeasy Mini Kit (QIAGEN GmbH, Hilden, Germany), and its amount and purity were confirmed by spectrophotometry. The RNase protection assay was performed with a commercial kit (Ambion). Briefly, [α-^{32}P]UTP-labeled probes were mixed with sample RNA and coprecipitated. Hybridization proceeded for 10 min at 68°C, followed by digestion of the unprotected RNA with RNase A-T1 for 30 min at 37°C and separation of the hybridized RNA on 5% acrylamide–8 M urea gels. The gels were dried on filter paper in a gel dryer (Bio-Rad) and exposed to X-ray film. Autoradiographs were scanned using an AlphaImager 2200 spot densitometer (Alpha Innotech Corporation), and the integrated densities of areas were recorded.

Northern blotting. Total RNA was isolated by using the RNeasy Mini Kit (QIAGEN GmbH) according to the manufacturer's instructions. Purity and yield were confirmed by spectrophotometry at 260 and 280 nm. Ten micrograms of RNA was denatured and separated on formaldehyde-containing 1.2% agarose gels by electrophoresis, blotted onto nylon membranes (Amersham), and probed with a ^{32}P-labeled osteopontin cDNA probe (generated by PCR using forward primer 5′-GCGAATTCTGGCTTATGGACTGAGGTC-3′ and reverse primer 5′-ATGGATCCGGAACTGTGTTTTTGCCTC-3′) or a 36B4 cDNA probe (generously provided by Goberdhan Dimri). Hybridization of the probe to the RNA was allowed to proceed overnight, and the membranes were washed and exposed to X-ray film at −80°C before development.

Immunoblot assay. For analysis of secreted osteopontin, the growth factor-deprived cell culture supernatant was collected from each treatment group. Forty microliters of supernatant per sample was electrophoresed on sodium dodecyl sulfate (SDS)–10% polyacrylamide minigels with nonreducing sample buffer. For analysis of intracellular proteins, cells were lysed in radioimmunoprecipitation assay buffer (50 mM Tris-HCl [pH 7.5], 150 mM NaCl, 1% NP-40, 0.5% sodium deoxycholate, 0.1% SDS) for the osteopontin blot or Akt kinase blot or in NP-40 buffer (150 mM NaCl, 1 mM EDTA, 20 mM Tris-HCl [pH 8.0], 0.5% NP-40) for the phospho-Akt blot. Cell lysates at equal amounts of protein (10 to 20 μg/lane) were electrophoresed on reducing SDS–10% polyacrylamide gels. The separated proteins were transferred to Pure Nitrocellulose membranes (Osmonics Inc.) and probed with antibodies to osteopontin (R&D Systems), Akt, and Akt phosphorylated at Ser473 (New England Biolabs, Beverly, Mass.). Detection was accomplished with the ECL chemiluminescence reagent.

Reporter assays. Comma-D cells stably transfected with vector, wild-type Akt, or constitutively active Akt were plated at 5×10^5 cells per 60-mm-diameter petri dish and grown for 24 h before transfection with Fugene. Various reporter constructs containing the luciferase reporter gene under the control of truncation mutants of the osteopontin promoter were used at 2 μg per transfection. The common internal transfection standard pRL-SV40 (10 ng per transfection) served as a control for transfection efficiency. Twenty-four hours after transfection, the cells were harvested in 0.4 ml of reporter lysis buffer (Promega), and dual luciferase reporter assays were performed by following the protocol provided by the manufacturer. Forty microliters of lysate was used for measurement in a luminometer (Turner Designs TD-20/20). Three separate experiments were performed, and results were calculated as means ± standard deviations. The lengths of the osteopontin promoter fragments tested were −88 to +79, −258 to +79, −472 to +79, −600 to +79, −777 to +79, and −882 to +79 (23).

DNA constructs and infection. The constructs of Akt kinase, constitutively active Akt kinase, and dominant-negative Akt kinase (K179M) in the pCMV-6 vector or in the retrovirus vector pLNCX were generously provided by Thomas Franke (12, 32) (the constitutively active Akt kinase was recloned into pLNCX in our laboratory). The construct for expression of the mouse osteopontin coding sequence was obtained by reverse transcription-PCR from osteosarcoma cells by using the sense primer 5′-ATGGATCCCGACCATGAGATTGGCAG-3′ and the antisense primer 5′-GCGAATTCGGACTGTGTTTTTGCCTC-3′. The resultant *Bam*HI-*Eco*RI cDNA fragment was ligated into the retrovirus vector pBabe. The construct for expression of osteopontin antisense, a full-length murine osteopontin cDNA generated by PCR, was ligated in the antisense orientation into the *Eco*RI and *Bam*HI sites of pBabe. The integrity of all constructs was confirmed by DNA sequencing.

The packaging cell line tsa54 was used to generate high-titer retrovirus (16) for infection of all breast epithelial cell lines. Ten micrograms of each retrovirus construct in conjunction with 10 μg of the pIK packaging vector was transfected into tsa54 cells by the calcium phosphate coprecipitation method, and the culture supernatant was collected on the day following transfection. In order to generate stable Akt transfectants, the murine breast tumor cell lines were infected with virus-containing supernatants in the presence of 8 μg of Polybrene (Sigma)/ml. Infected cells were selected in MECL medium with G418 (200 to 500 μg/ml). For double infection, cells expressing constitutively active Akt or mutant Akt were infected with plasmids encoding sense or antisense osteopontin. Forty-eight hours later, selection with puromycin (2 to 4 μg/ml) commenced for 5 days, followed by analysis of RNA and protein expression. Several clones were selected and characterized for all single infectants, while the doubly transduced cells were selected and analyzed in bulk.

Cell motility. The cell motility experiment is often referred to as an in vitro wounding assay (21, 27) because a cell monolayer is disrupted and the rate of repopulation is assessed. Breast epithelial cells were plated at 2.5×10^5 per 100-mm-diameter petri dish. After 2 days, they were grown in growth factor-deprived medium for 24 h. The cultured cells were disrupted by scratching with a pipet aid equipped with a 1,000-μl tip. Repopulation of the cell-free area was examined under an inverted microscope after 22 h. In this time frame, cell division is negligible in growth factor-deprived medium.

Soft-agar growth. Cells (5×10^5 per 60-mm-diameter dish) were plated in triplicate with a top layer of 0.3% agar (Bacto Agar; Difco, Detroit, Mich.) and a bottom layer of 0.5% agar (both in MECL medium). Every other day, 0.3 ml of MECL medium was supplemented and the plates were examined microscopically for growth. After 3 weeks, the number of cell clusters per microscopic field and the number of cells per cluster were counted in five views per plate (one central, four peripheral), and cell clusters were photographed. Soft-agar assay conditions have not been standardized because they depend on the specific cell lines under study. The size of the cell clusters obtained differs widely with the cell lines used; cell clusters may comprise fewer than 10 cells (7, 25) or reach microscopically (36) or macroscopically (43) visible diameters. For Comma-D cells transfected with Akt, an incubation time of 3 weeks before enumeration has been found suitable (40). We chose to determine the frequency of clones formed and the clone size (numbers of cells per cluster). At the plating density and within the time frame employed here, this quantitation could be performed accurately, and the resulting histograms of cluster size and frequency were considered to be more informative than the simple enumeration of clusters above a randomly chosen size. The resulting histograms are characteristic of the individual cell lines and were analyzed for statistical differences in variance by the F-test, by accepting a probability of error of 1, 5, or 10% with a one-sided paired comparison.

In vivo tumorigenesis. MT2994 cells or FSK-7 cells were harvested by trypsinization. A total of 0.5×10^6 cells in 0.5 ml of phosphate-buffered saline

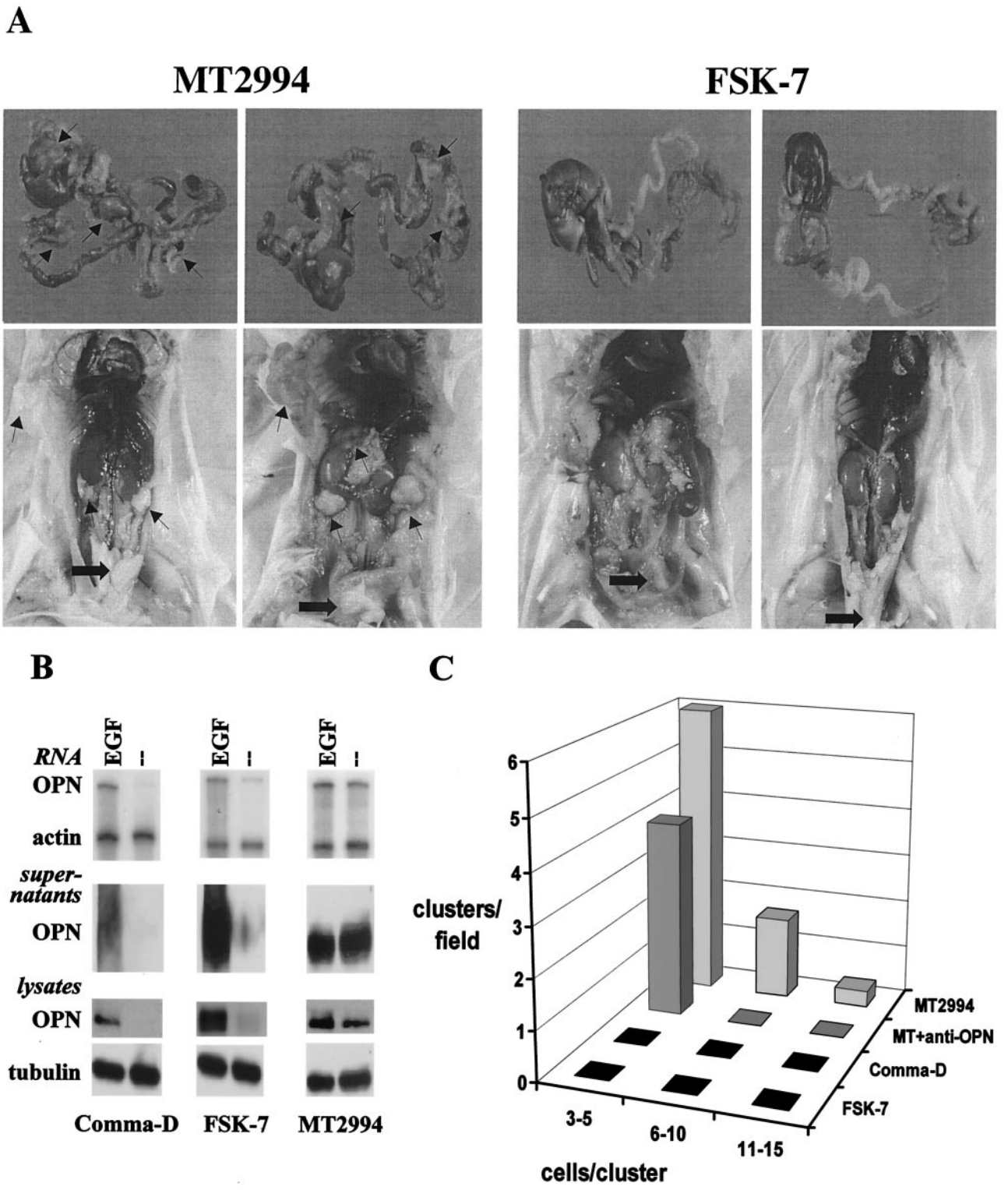

FIG. 1. Constitutive osteopontin expression contributes to a malignant phenotype in breast tumors. (A) MT2994 cells or FSK-7 cells (0.5×10^6) were injected orthotopically into the left inguinal mammary fat pads of BALB/c mice. After 21 days, the mice were analyzed for tumor formation and metastasis. The upper panel shows the livers and gastrointestinal tracts; the lower panel depicts the opened abdomens. Arrows point to metastases. Thick arrows indicate the primary tumors (in MT2994 cells) or hyperplasias (in FSK-7 cells). These results are representative for 10 mice in each group. (B) Cells were maintained under growth factor-deprived conditions in the presence or absence of EGF for 14 h. Supernatants were collected, and cells were lysed. Osteopontin (OPN) expression was assessed on the RNA level by an RNase protection assay (using β-actin as a loading control) and on the protein level by Western blotting (using tubulin as a loading control for the cell lysates). (C) MT2994 cells (5×10^5 cells/60-mm-diameter petri dish) were grown in soft agar in the absence of antibodies (back row, MT2994) or in the presence of an anti-osteopontin antibody (third row from front, MT + anti-OPN) for 21 days. The frequency of clone formation and clone size (number of cells per cluster) were enumerated in five random microscopic fields. While control immunoglobulin had no effect (data not shown), the anti-osteopontin antibody suppressed clone formation. Comma-D cells and FSK-7 cells do not constitutively secrete osteopontin and do not form clones in soft agar when grown under identical conditions (front rows, FSK-7 and Comma-D).

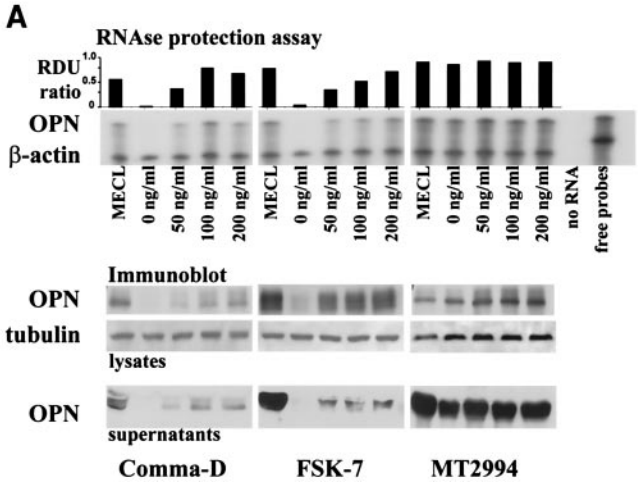

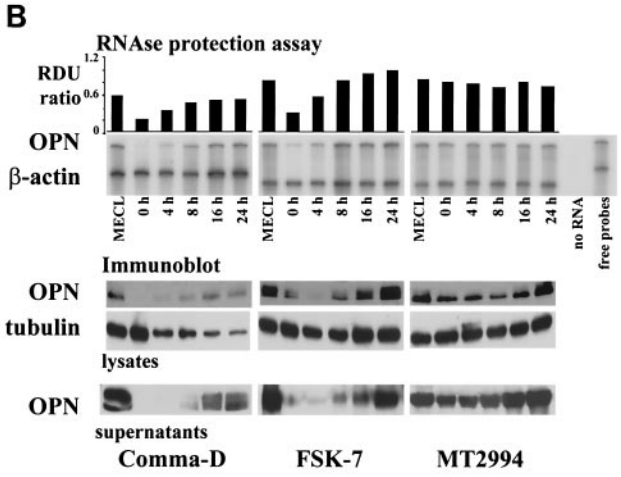

FIG. 2. EGF-mediated signaling induces osteopontin in benign but not in malignant breast epithelial cells. A total of 5×10^5 cells were plated in 6-well plates for 7 h. Following serum starvation for 14 h, the transformed breast epithelial cells were stimulated dose dependently at 24 h (A) or time dependently at 100 ng/ml (B) with EGF. MECL, normal growth medium containing 2% adult bovine serum, EGF, and insulin. Osteopontin (OPN) expression was analyzed by an RNase protection assay on total RNA. The results were confirmed by analysis on the protein level by immunoblotting of cell lysates and supernatants. Tubulin and β-actin served as loading controls, respectively. RDU ratio, relative density units of osteopontin RNA divided by relative density units of actin RNA. (C) Quantitation of total osteopontin in culture 24 h after treatment with increasing amounts of EGF. (D) Comma-D cells and MT2994 cells were grown on coverslips in the presence or absence of growth factors. The cells were stained with fluorescently labeled antibodies to actin (FITC; green) or osteopontin (phycoerythrin; red). Nuclei were stained with DAPI (blue). No nonspecific signal was detected after incubation with streptavidin-phycoerythrin in the absence of the antiosteopontin antibody. Likewise, a nonspecific FITC-labeled antibody did not visibly stain the cells (data not shown).

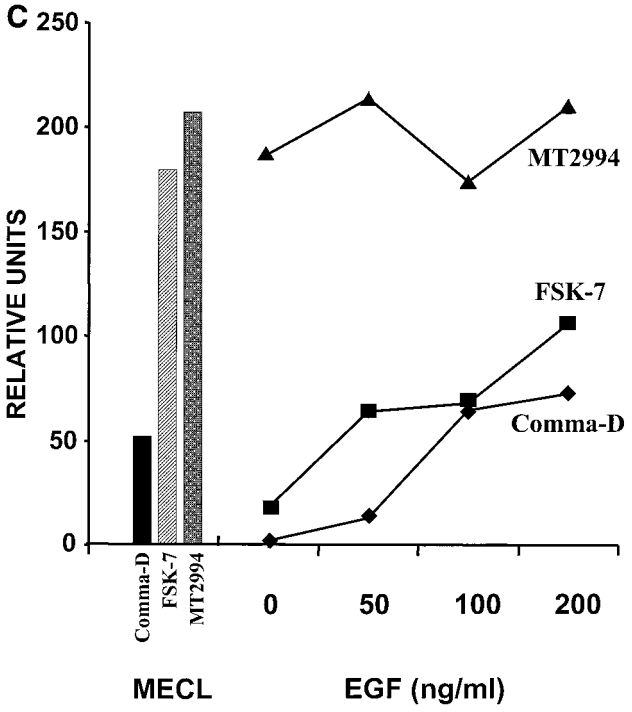

were injected orthotopically into the left inguinal mammary fat pads of female BALB/c mice (age, 8 to 10 weeks). After 21 days, the animals were sacrificed and necropsy was performed for the detection of primary tumors or hyperplasia and metastases. To ascertain that the FSK-7 cells were free of murine pathogens, serum samples from injected animals were tested for Sendai virus, pneumonia virus of mice, mouse hepatitis virus, minute virus of mice, Theiler's murine encephalomyelitis virus, reovirus, *Mycoplasma pulmonis*, mouse parvovirus, epizootic diarrhea of infant mice virus, lymphocytic choriomeningitis virus, mouse adenovirus, ectromelia (mousepox virus), K virus, polyomavirus, mouse thymic virus, mouse cytomegalovirus, hantavirus, *Encephalitozoon cuniculi*, and cilium-associated respiratory bacillus. Results of serological testing were negative in all instances. The in vivo experiments were performed under a protocol approved by the institutional animal care and use committee at Tufts-New England Medical Center.

RESULTS

The malignant phenotype is associated with constitutive osteopontin expression in breast tumor cells. MT2994 cells formed disseminating tumors after orthotopic injection, whereas FSK-7 cells showed modest local growth, diagnosed as hyperplasia, that did not develop into tumors and did not spread beyond the site of injection (Fig. 1A). Comma-D cells and FSK-7 cells secreted osteopontin in EGF-containing medium. Under growth factor-deprived conditions, no osteopontin RNA or protein expression was detectable. In contrast, MT2994 cells had high constitutive levels of osteopontin, regardless of the presence or absence of growth factors (Fig. 1B). Soft-agar colony formation measures the ability of cells to grow independently of anchorage and correlates well with the capacity of tumor cells for invasiveness in vivo (55). We hypothesized that the importance of osteopontin for the dissemination of breast cancer cells would also be reflected in an essential contribution by this molecule to soft-agar colony formation. In initial experiments, we asked whether malignant cells form clones in soft agar in an osteopontin-dependent fashion. As expected, the benign Comma-D and FSK-7 cells did not form clones under these conditions. MT2994 cells formed clones in soft agar in a manner that was specifically inhibitable by addition of an antiosteopontin antibody (Fig. 1C). Hence, we set out to analyze the molecular mechanisms of osteopontin induction in breast cancer cells.

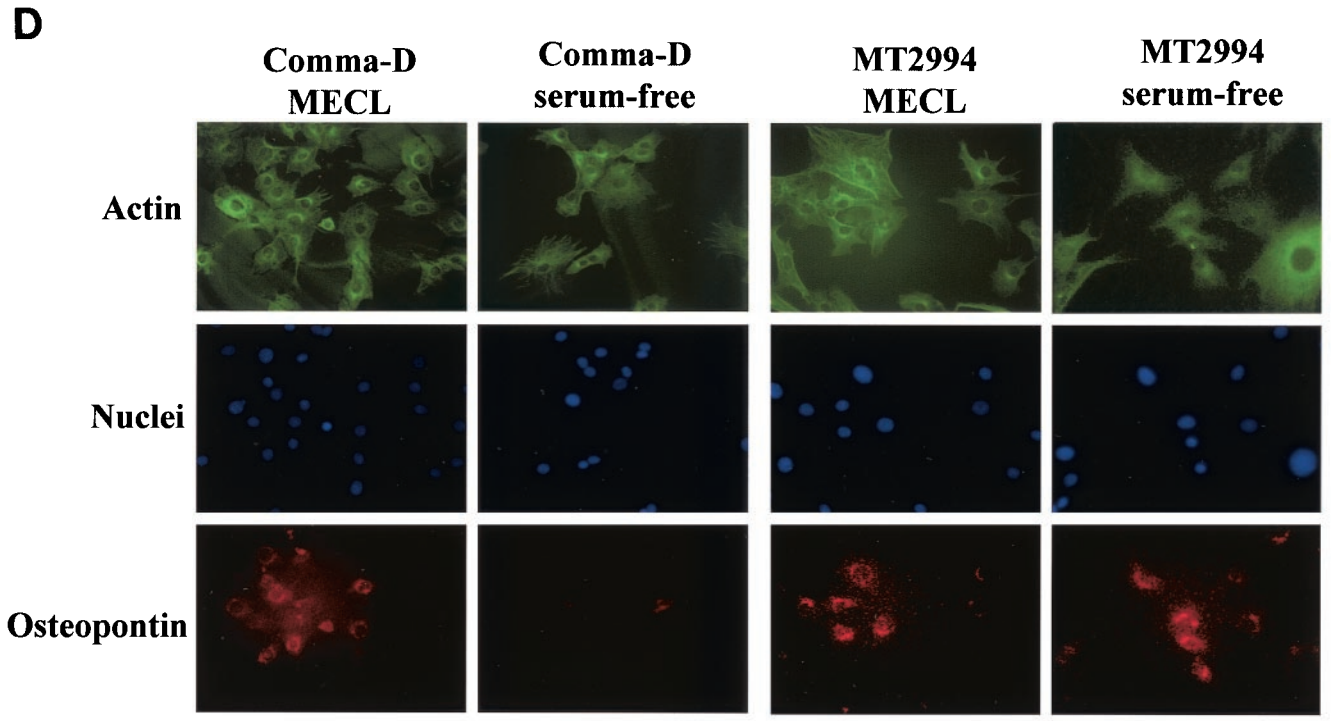

FIG. 2—*Continued.*

Osteopontin gene expression is linked to the activation of growth factor signaling. We asked whether osteopontin gene expression by breast tumor cells is secondary to activation of growth factor signaling pathways. The elimination of growth factors from the medium reduced the expression of osteopontin in the benign breast epithelial cell lines Comma-D and FSK-7 but not in the malignant breast tumor line MT2994. Conversely, stimulation of the cells with EGF induced osteopontin expression in Comma-D cells and FSK-7 cells in a time- and dose-dependent manner but did not affect osteopontin expression in MT2994 cells. (Fig. 2A and B). To quantitate this observation, we performed densitometry of osteopontin on the Western blots of cell lysates and supernatants and calculated the total amounts of osteopontin protein per cell culture dish (5×10^5 cells) consecutive to the titration of EGF. At 200 ng of EGF/ml over 8 h, the levels of osteopontin expression in Comma-D cells and FSK-7 cells are about one-half of those in MT2994 cells. In the latter cell line, the osteopontin expression levels are not further induced by EGF (Fig. 2C).

Differences in osteopontin expression between the benign and malignant cell lines were also confirmed by fluorescent microscopy with a biotinylated anti-osteopontin antibody (R&D Systems) and streptavidin-phycoerythrin. The nuclei were stained with 4′,6′-diamidino-2-phenylindole (DAPI), and the cytoplasm was stained with fluorescein isothiocyanate (FITC)-conjugated anti-β-actin. The signal for osteopontin was constitutive in MT2994 cells in growth factor-deprived medium and was not further enhanced by the addition of exogenous EGF. In contrast, Comma-D cells and FSK-7 cells (data not shown) depended on the addition of growth factors in the medium for significant osteopontin staining (Fig. 2D). The location of the osteopontin signal was predominantly perinuclear, which is characteristic of secreted proteins (15).

The constitutive osteopontin expression in malignant breast epithelial cells correlates with a gain of function in the PI 3-kinase pathway. We analyzed the involvement of signal transduction molecules associated with the EGF receptor in the induction of osteopontin gene expression. Addition of the PLC inhibitor U73122 or the PI 3-kinase inhibitor wortmannin reversed the EGF-mediated increase in osteopontin mRNA levels in Comma-D and FSK-7 cells. In contrast, the high abundance of osteopontin mRNA in MT2994 cells remained unaffected by either inhibitor (Fig. 3A).

Because wortmannin could not reverse the constitutive osteopontin gene expression in MT2994 cells, the defect leading to its up-regulation was likely to be downstream of PI 3-kinase. PI 3-kinase can phosphorylate and activate Akt kinase. In malignant cells, Akt kinase activity may be elevated due to phosphorylation on serine 473 and threonine 308. We therefore tested Akt phosphorylation in the breast tumor cells on Western blots with a phospho-Akt-specific antibody. Stripping and reprobing for total Akt kinase and for tubulin served as controls for Akt expression levels and for equal loading of the gels, respectively. Akt was constitutively phosphorylated in the malignant cell line MT2994 but not in Comma-D or FSK-7 cells, where Akt kinase phosphorylation was EGF induced and transient. This is not accounted for by overexpression of the kinase, because levels of total Akt were not higher in MT2994 cells than in Comma-D or FSK-7 cells (Fig. 3B).

Overexpression of Akt kinase induces osteopontin gene expression. To gain further mechanistic insight into the contributions by Akt kinase to osteopontin gene expression, we sta-

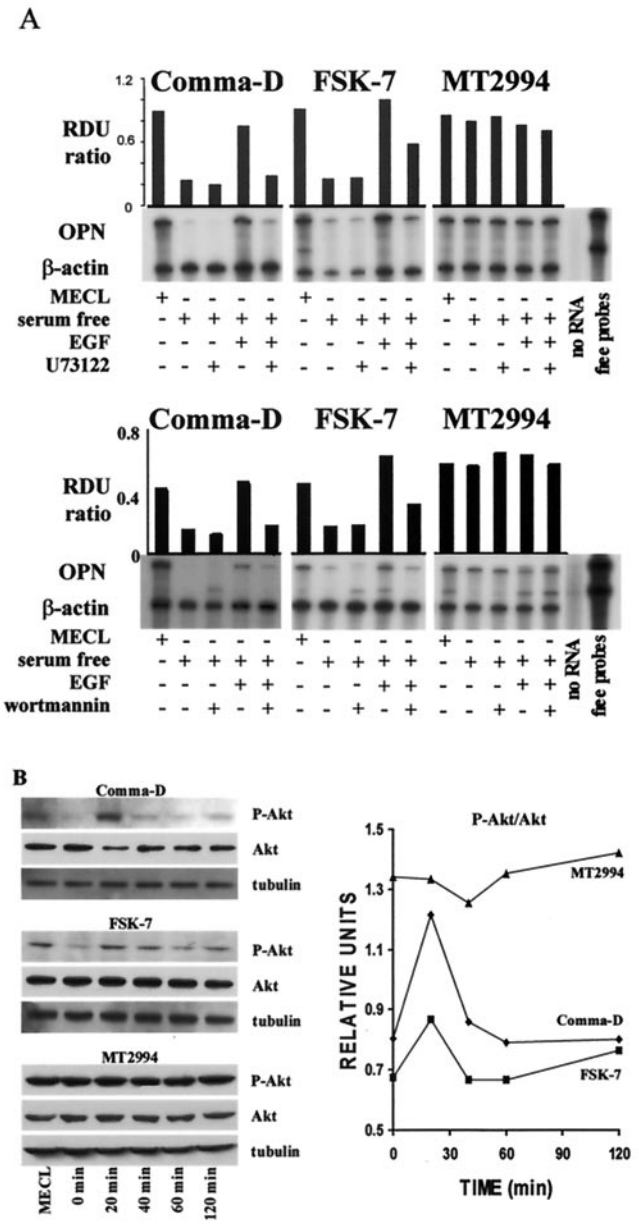

FIG. 3. Osteopontin expression depends on the PI 3-kinase pathway in breast epithelial cells. (A) The PLC inhibitor U73122 or the PI 3-kinase inhibitor wortmannin was used in growth factor-deprived medium to assess EGF-dependent signal transduction leading to osteopontin gene expression. Wortmannin (100 nM) was added to the cells before incubation in the presence or absence of 100 ng of EGF/ml for 8 h. Similarly, U73122 was added to the cells at a final concentration of 500 nM. Osteopontin gene expression was analyzed by an RNase protection assay on total RNA and standardized by comparison to β-actin. (B) Phosphorylation of Akt kinase in breast epithelial cells. A total of 5×10^5 cells were seeded in 6-well plates for 7 h. Following serum starvation for 14 h, they were incubated for the indicated times in growth factor-deprived medium with 100 ng of EGF/ml. The cells were harvested and lysed, and 20 μg of lysate was probed by immunoblotting with antitubulin, anti-Akt, and anti-phospho-Akt antibodies. (Left panel) Immunoblots; (right panel) spot densitometry (integrated density values) for phospho-Akt (P-Akt)/Akt.

bly transduced the breast epithelial cells with various Akt kinase constructs. Comma-D cells were transfected with vector, wild-type Akt, or constitutively active Akt. FSK-7 cells were transfected with vector or constitutively active Akt. MT2994 cells were transfected with vector, wild-type Akt, or a dominant-negative Akt mutant. The expression levels of the transfected genes were measured on the RNA and protein levels. As expected, osteopontin was constitutively expressed in Akt kinase-transduced Comma-D cells and FSK-7 cells, while the constitutive osteopontin gene expression in MT2994 cells was suppressed by the dominant-negative Akt kinase mutant, as shown by an RNase protection assay and Western blotting (Fig. 4A). We confirmed the osteopontin message levels by Northern blotting (with 36B4 as a loading control) and found this measurement to be in good correlation with the RNase protection assay results (Fig. 4B). The levels of osteopontin induced by wild-type Akt and constitutively active Akt are comparable, likely reflecting the substantial overexpression of Akt kinase. At these amounts, the baseline activity of wild-type Akt kinase is sufficient to transduce a signal. It should be noted that the reduction of osteopontin gene expression by dominant-negative Akt kinase is partial. Only moderate levels of overexpression can be achieved for dominant-negative Akt kinase, because this mutant also slows down cell division (compare Fig. 5B below), consistent with the hypothesis that the constitutive activation of Akt kinase in MT2994 cells is causative for the transformation of these cells.

Previous studies have shown that the induction of osteopontin in renal epithelial cells by transforming growth factor β or EGF is caused by increased transcription (34). Akt kinase activity has previously been associated with activation of the AP-1 transcription factor and Ets family transcription factors (17, 18, 28), both of which are known to bind to the osteopontin promoter (reviewed in reference 52). We set out to further map the molecular connections between Akt kinase activity and osteopontin transcription in breast epithelial cells. For this purpose, we took advantage of the breast epithelial cell lines constitutively expressing various Akt constructs that we had generated. We used Comma-D cells stably expressing wild-type Akt kinase, constitutively active Akt kinase, or vector in luciferase reporter assays under the control of full-length or truncated osteopontin promoter sequences. As expected, Akt kinase activity can induce the transactivation of the osteopontin promoter (Fig. 4C). The Akt-responsive promoter domain was mapped to a region between base −600 and base −777. Consistent with a previous report (23), a far-distal promoter element (between bases −777 and −882) appeared to contain a repressor.

Akt kinase enhances the growth rate through osteopontin-independent pathways and mediates migration through osteopontin. In order to differentiate between osteopontin-dependent and osteopontin-independent consequences of Akt kinase overexpression, we generated doubly transduced lines. FSK-7 cells that stably expressed constitutively active Akt kinase were infected with a retrovirus containing osteopontin antisense, yielding FSK-7 vector plus vector, FSK-7 constitutively active Akt plus vector, and FSK-7 constitutively active Akt plus antisense osteopontin cells. Similarly, we generated MT2994 vector plus vector, MT2994 dominant-negative Akt plus vector, and MT2994 dominant-negative Akt plus os-

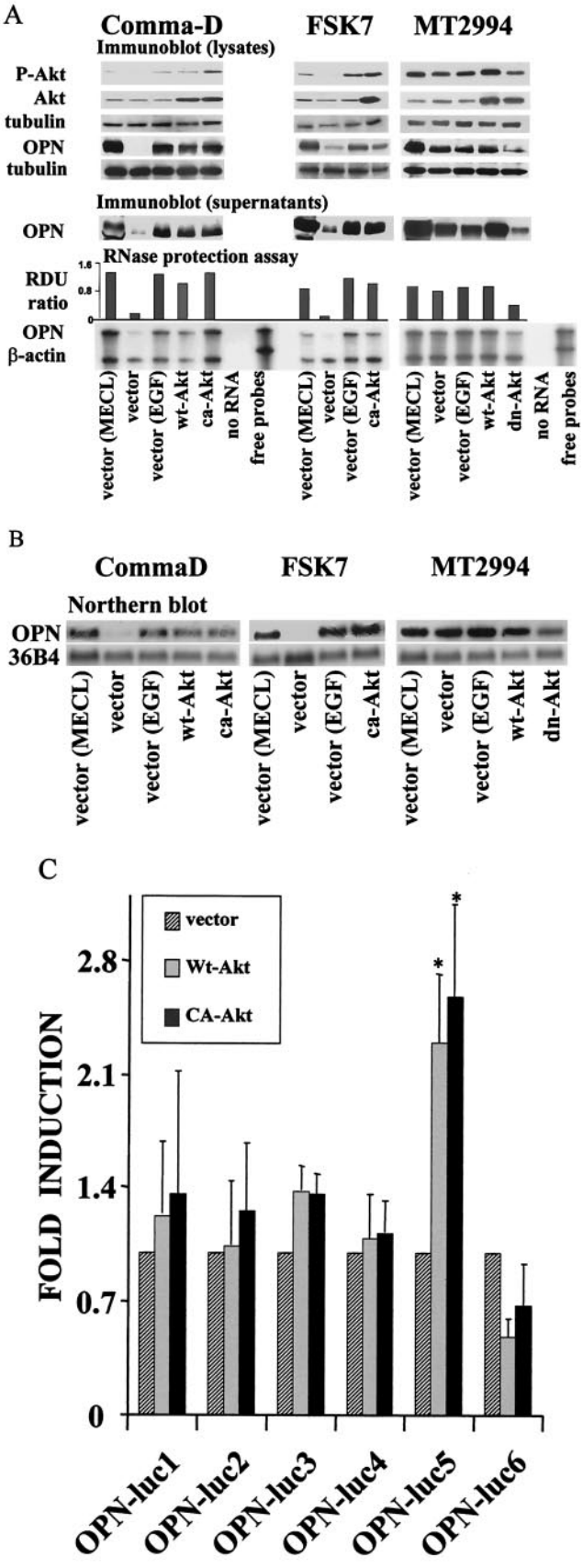

teopontin cells. As before, the expression levels of the modulated genes were measured by Western blotting. The elevated osteopontin expression in transfectants of constitutively active Akt kinase could be reversed by cotransfection of antisense osteopontin, and the suppression of osteopontin by dominant-negative Akt was reversed by cotransfection with the osteopontin gene (Fig. 5A).

We tested the growth rates of doubly transduced cells by plating 5,000 cells per well in 24-well plates, followed by daily cell counts in quintuplicate. Remarkably, within only 1 day, transfection of constitutively active Akt kinase into FSK-7 cells significantly induced the growth rate, while transfection of dominant-negative Akt kinase into MT2994 cells significantly reduced it. The differences remained significant throughout the 4 days of measurement. In contrast, the stable transfection of osteopontin into cells overexpressing dominant-negative Akt kinase or of osteopontin antisense into cells overexpressing constitutively active Akt kinase had no effect on the growth rates (Fig. 5B). Identical results were obtained with singly transduced FSK-7 cells expressing constitutively active Akt kinase and MT2994 cells expressing dominant-negative Akt kinase (data not shown).

We also analyzed cell motility in vitro. Doubly transduced FSK-7 cells were plated at 2.5×10^5 per 100-mm-diameter dish and grown for 2 days. They were starved for 24 h in growth factor-deprived medium. The geometry of the cell culture was

FIG. 4. Akt kinase activity induces osteopontin gene expression. (A) Following serum starvation for 14 h, the transfected breast epithelial cells were grown under growth factor-deprived conditions, stimulated by EGF, or kept in normal growth medium containing 2% adult bovine serum, EGF, and insulin (MECL). Osteopontin (OPN) expression was analyzed by an RNase protection assay, and a probe for β-actin was used to control for loading. RDU ratio, relative density units of osteopontin RNA divided by those of actin RNA. The results were confirmed by analysis on the protein level by immunoblotting of cell culture supernatants. Overexpression of the transfected Akt constructs was confirmed by Western blotting using cell lysates. Lysates from transiently transfected 293T cells confirmed the integrity of the transfected DNA constructs (data not shown). The levels of resulting Akt phosphorylation were tested with a phospho-Akt (P-Akt)-specific antibody. Tubulin served as a loading control. wt-Akt, wild-type Akt; ca-Akt, constitutively active Akt; dn-Akt, dominant-negative Akt. (B) The results from the RNA protection assay were confirmed by Northern blotting on total RNA from cells transfected with various Akt constructs (ca-Akt, wt-Akt, and dn-Akt). The cells had been cultured in complete medium (MECL) or in serum-free medium with or without EGF. The blot was probed for osteopontin and for 36B4 (loading control). Similar results were obtained with additional clones of ca-Akt-transfected FSK-7 cells and dn-Akt-transfected MT2994 cells (data not shown). (C) Reporter assays with osteopontin promoter constructs. Comma-D cells stably expressing wild type Akt kinase (Wt-Akt), constitutively active Akt kinase (CA-Akt), or the vector control were transiently transfected with luciferase (luc) reporter constructs under the control of various fragments of the osteopontin promoter. The lengths of the osteopontin promoter truncation mutants tested were −88 to +79 (OPN-luc1), −258 to +79 (OPN-luc2), −472 to +79 (OPN-luc3), −600 to +79 (OPN-luc4), −777 to +79 (OPN-luc5), and −882 to +79 (OPN-luc6). With OPN-luc5, the data for Wt-Akt and for CA-Akt are significantly different from the data for the vector control ($P < 0.05$ [asterisked] according to the t test for paired samples, after testing for normal distribution and equal variance). Luciferase activity is expressed in relative units, with the activity of the vector-transduced Comma-D cells set at 1. Data reflect averages of three independent experiments. Error bars, standard deviations.

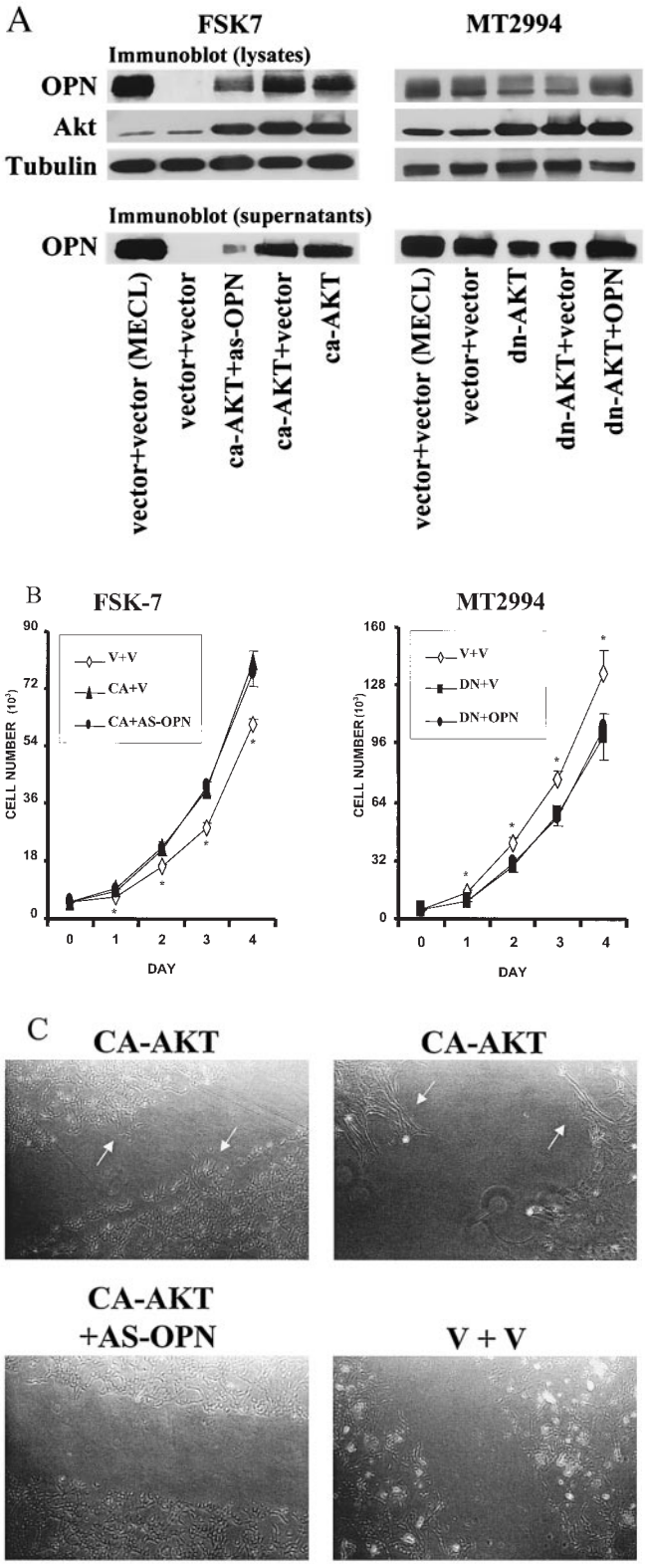

FIG. 5. Osteopontin is a downstream effector of Akt kinase for migration but not for growth. (A) After serum starvation for 14 h, transfected breast epithelial cells were grown under growth factor-deprived conditions or kept in normal growth medium (MECL). Overexpression of the transfected constructs was confirmed by Western blotting using cell lysates and cell culture supernatants from transduced FSK-7 or MT2994 cells. Expression of the transfected Akt constructs was analyzed by Western blotting with antihemagglutinin or anti-Akt kinase. Tubulin served as a loading control. Osteopontin expression levels were measured by probing blots of cell lysates and supernatants with a specific antiosteopontin antibody. ca-Akt, constitutively active Akt kinase; dn-Akt, dominant-negative Akt kinase; OPN, osteopontin; as-OPN, osteopontin antisense. (B) Akt kinase induces cell growth independently of osteopontin. Cells were plated at 5×10^3 per well in 24-well plates. Cell numbers per well were determined daily using a Coulter Z Series cell counter. Each data point represents the mean ± standard deviation of five measurements. Data points labeled with an asterisk are significantly different ($P < 0.05$) from the other data sets. V, vector transfectant; CA, transfectant of constitutively active Akt kinase; DN, transfectant of dominant-negative Akt kinase; OPN, transfectant of osteopontin; AS-OPN, transfectant of osteopontin antisense). (C) Constitutive osteopontin expression is necessary for cell motility. Transduced FSK-7 cells were plated at 2.5×10^5 per 100-mm-diameter dish. After 2 days, they were grown in growth factor-deprived medium for 24 h. The cultured cells were disrupted by scratching with a pipet aid equipped with a 1,000-μl tip. Repopulation of the cell-free area was examined under an inverted microscope after 22 h. Transfectants with constitutively active Akt (CA-AKT) sprout into the depleted area (arrows, top left). A higher magnification shows the reorientation of the cells (arrows, top right). No substantial changes are seen in cells transduced with constitutively active Akt plus antisense osteopontin (CA-AKT + AS-OPN) (bottom left) or vector controls (V + V) (bottom right). Similar results were obtained in three additional experiments.

disturbed by scratching across the diameter of the cell culture dish. After 22 h, FSK-7 cells transfected with constitutively active Akt displayed reorientation and migration into the space between the continuous layers. Cotransfected osteopontin antisense completely reversed this effect, and like cells transfected with the vector control, these cells did not move (Fig. 5C). For a more quantitative analysis of cell motility, we performed a transwell chamber chemokinesis assay with coating of both sides of the membrane with 10 μg of fibronectin/ml. A total of 2.5×10^4 cells were placed in the upper chamber, and serum- and growth factor-free medium was placed in both compartments. After 4 h, the numbers of cells per optical field on the lower side of the membrane were 9 ± 2 for FSK-7 vector plus vector, 19 ± 6 for FSK-7 vector plus antisense osteopontin, 51 ± 2 for FSK-7 constitutively active Akt plus vector, and 32 ± 4 for FSK-7 constitutively active Akt plus antisense osteopontin. These results are consistent with osteopontin-independent roles of Akt as a growth-promoting gene product and osteopontin-dependent roles of Akt as a migration-promoting gene product.

Osteopontin-dependent and -independent pathways contribute to generating a malignant phenotype. Because osteopontin is necessary for soft-agar colony formation (see Fig. 1C) and Akt kinase induces osteopontin expression, we asked whether the constitutive overexpression of Akt kinase in FSK-7 cells was sufficient to confer anchorage-independent growth. As expected, Akt-transfected FSK-7 cells displayed clone formation in soft agar, whereas vector-transfected FSK-7 cells did not. The repeated addition of an anti-osteopontin antibody to the cell culture reduced the numbers and sizes of clones formed. In contrast, a control immunoglobulin had no effect (Fig. 6A). As in the preceding experiment (compare Fig. 1C), the inhibition of clone formation by an antiosteopontin antibody was partial, a finding which may reflect limitations in the neutralization by the antibody. We therefore analyzed the dou-

bly transduced cells for colony formation in soft agar. Coexpression of osteopontin antisense in FSK-7 cells expressing constitutively active Akt led to a partial reduction in colony formation. Consistent with the earlier results, FSK-7 cells transduced with vector constructs did not form clones in soft agar (Fig. 6B). In a complementary approach, expression of dominant-negative Akt in MT2994 cells caused a partial reduction in the numbers and sizes of clones formed (a shift of the histogram to the left), consistent with the partial suppression of Akt kinase activity by the dominant-negative construct. Coexpression of osteopontin virtually completely reversed this inhibition (Fig. 6C). The differences among the transduced MT2994 cells did not reach statistical significance, which is likely due to the incomplete suppression of endogenous Akt activity by the dominant-negative construct. Dominant-negative variants of essential growth-promoting gene products can typically be overexpressed only at moderate levels (1). Residual Akt activity has previously been observed after transfection with the Akt (K179M) construct (12, 32).

We tested in vivo tumorigenesis and dissemination by using doubly transduced FSK-7 cells. As expected, cells transduced with vector plus vector or with vector plus antisense osteopontin generated small hyperplastic lesions. In contrast, cells expressing constitutively active Akt generated larger tumors. Only the FSK-7 cells containing Akt plus vector, not the FSK-7 cells expressing Akt plus antisense osteopontin, formed distal lesions (Fig. 7). These experiments were extended to 30 days (at that time point, equal numbers of MT2994 cells are lethal), and the distal foci formed were smaller than those observed with MT2994, suggesting that additional factors may contribute to MT2994 malignancy. However, the observations are consistent with a critical role of Akt kinase in tumor growth and dissemination, the latter being mediated by high constitutive levels of osteopontin.

DISCUSSION

The molecular processes that lead to dysregulated growth of cancer cells can be distinguished from the molecular mechanisms that mediate dissemination. Osteopontin mRNA expression and secretion by *ras*-transformed NIH 3T3 cells correlate with these cells' levels of *ras* expression and their metastatic ability (9, 10). In contrast, LTA cells transfected with *ras* or with *ras* plus v-*myc* decrease the expression of osteopontin and remain tumorigenic but nonmetastatic (13, 14, 37). Osteopontin is the physiologic ligand of CD44v6, which also mediates dissemination without altering tumor growth. Expression of the CD44 splice form containing the variant exon 6 on various tumor cells is necessary and sufficient to mediate metastasis formation. Overexpression of CD44v6 in nonmetastasizing pancreatic tumor cells was sufficient to establish full metastatic behavior (22). In a complementary approach, a monoclonal antibody to the metastasis-specific exon of CD44 retarded lymph node and lung colonization by a metastatic pancreas tumor line (44). In mice that are susceptible to carcinogenesis due to *p53* mutation, the absence of the *CD44* gene leads to abolishment of osteosarcoma metastasis but not to changes in tumor incidence or growth (54). Based on the phenotypes of mice with knockouts of various confirmed metastasis genes, including osteopontin and CD44, the genetic basis of metastasis formation has been identified as aberrant expression or splicing of a unique set of developmentally nonessential genes that physiologically mediate the homing of immune system cells (53).

Metastasis formation arises with consistent patterns of organ preference. It has not been clear how the primary defect of growth dysregulation is linked to the expression of specific metastasis genes. We have screened signal transduction molecules associated with the EGF receptor and have identified constitutive phosphorylation, indicative of activation, of Akt kinase in malignant, but not in benign growth-dysregulated, immortal breast epithelial cells. Akt kinase activity supports tumor growth as well as the induction of osteopontin, a metastasis gene that is essential for breast cancer dissemination to bone. Our results may provide a molecular explanation for the previous observation that transfection of Akt1 into immortalized, not fully transformed Comma-1D cells mediates, mutually independently, the transformation and invasion of breast epithelial cells (40). Human breast carcinogenesis is associated with a loss of cellular retinal-binding protein (CRBP) expression in about one-fourth of all cases. The inhibition of the PI 3-kinase/Akt kinase pathway by CRBP suppresses breast cancer cell survival and anchorage-independent growth (30). The latter is likely due to the inhibition of osteopontin gene expression. Elevated Akt kinase activity is also seen in metastasizing, but not in nonmetastasizing, liver tumor cells (36). Akt kinase has also been associated with the invasiveness of pancreas cancer, but here the pro-metastatic gene induced by Akt is the IGF-I receptor (48).

The cause for the constitutive activation of Akt kinase in MT2994 cells remains unknown. Activating mutations in Akt itself seem unlikely, because mutants with known activating amino acid changes, such as E40K, still respond to inhibition by wortmanin. The loss of negative regulators of Akt kinase may desensitize the enzyme and generate the appearance of PI 3-kinase independence. We have sequenced the mRNA of PTEN, the most prominent negative regulator of Akt, in MT2994 cells and FSK-7 cells (data not shown). No mutations were found in either case. Reduced expression levels of PTEN or a lack of other negative regulators are likely causes.

Our studies of murine transformed breast epithelial cells have indicated that constitutive activation of Akt kinase, independent of PI 3-kinase, causes a malignant phenotype through continuing cell cycle progression and expression of osteopontin (MT2994 cells). In contrast, breast epithelial cells may be immortalized through signal transduction that is independent of the EGF/PLC/PI 3-kinase/Akt kinase pathway (Comma-D cells and FSK-7 cells), but this transformation is not associated with osteopontin gene expression or with metastasis. Dysregulation of Akt kinase activity also plays a prominent role in human breast tumor cells. There, the constitutive activation of Akt kinase is typically secondary to overexpression of ErbB on the cell surface and is dependent on PI 3-kinase. Estrogen stimulates Akt activation, which is reflected in phosphorylation at serine 473 of the oncoprotein, in estrogen receptor-negative breast cancer cells. Activation of Akt by estrogen in these cells is time and dose dependent and can be blocked by inhibitors of PI 3-kinase and Src kinase but not by estrogen antagonists (49). The interdependent regulation between the estrogen receptor α and PI 3-kinase/Akt pathways may play an important role in

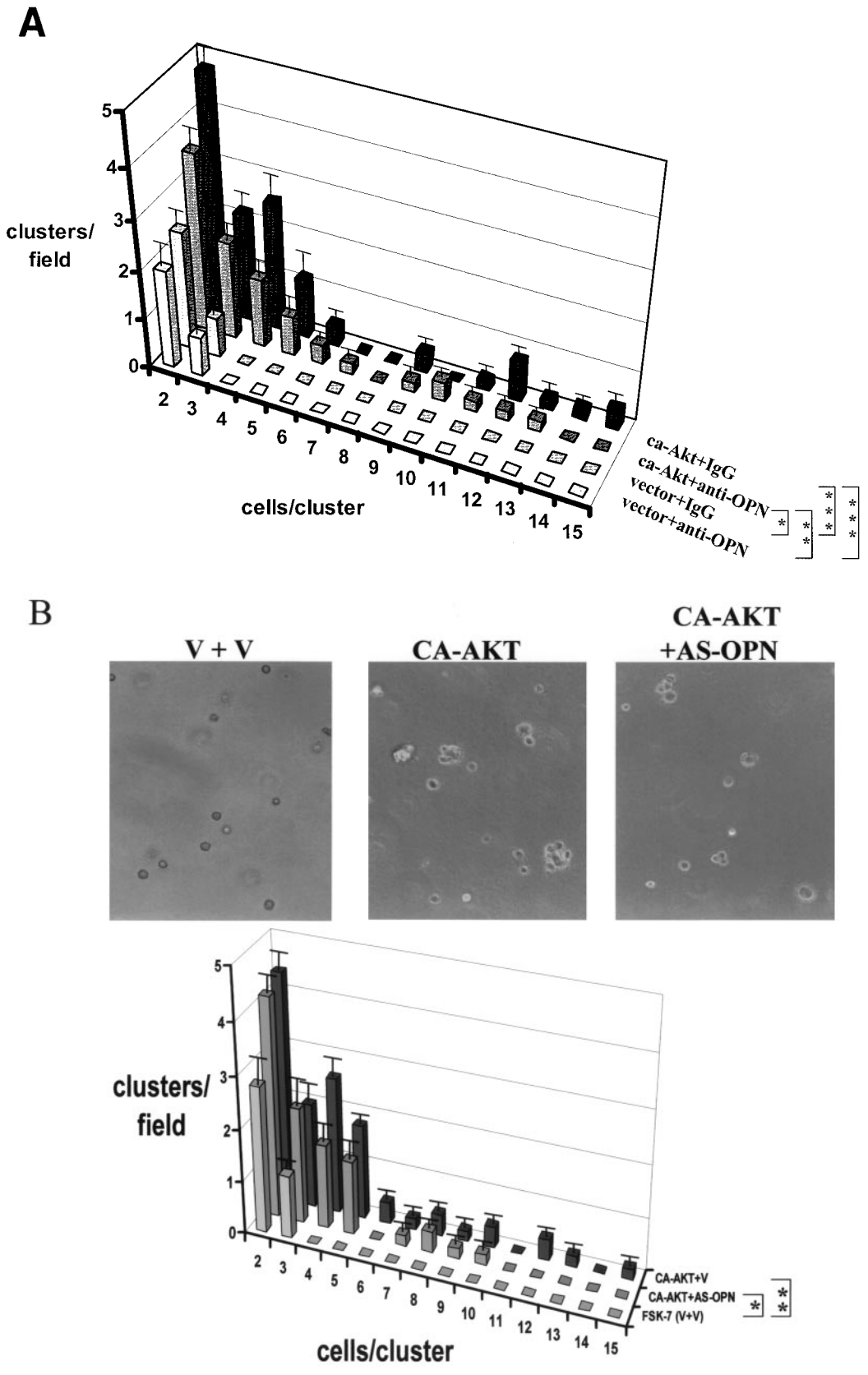
A
clusters/
field
0
1
2
3
4
5
2 3 4 5 6 7 8 9 10 11 12 13 14 15
cells/cluster
ca-Akt+IgG
ca-Akt+anti-OPN
vector+IgG
vector+anti-OPN
B
V + V
CA-AKT
CA-AKT
+AS-OPN
clusters/
field
0
1
2
3
4
5
2 3 4 5 6 7 8 9 10 11 12 13 14 15
cells/cluster
CA-AKT+V
CA-AKT+AS-OPN
FSK-7 (V+V)

FIG. 6

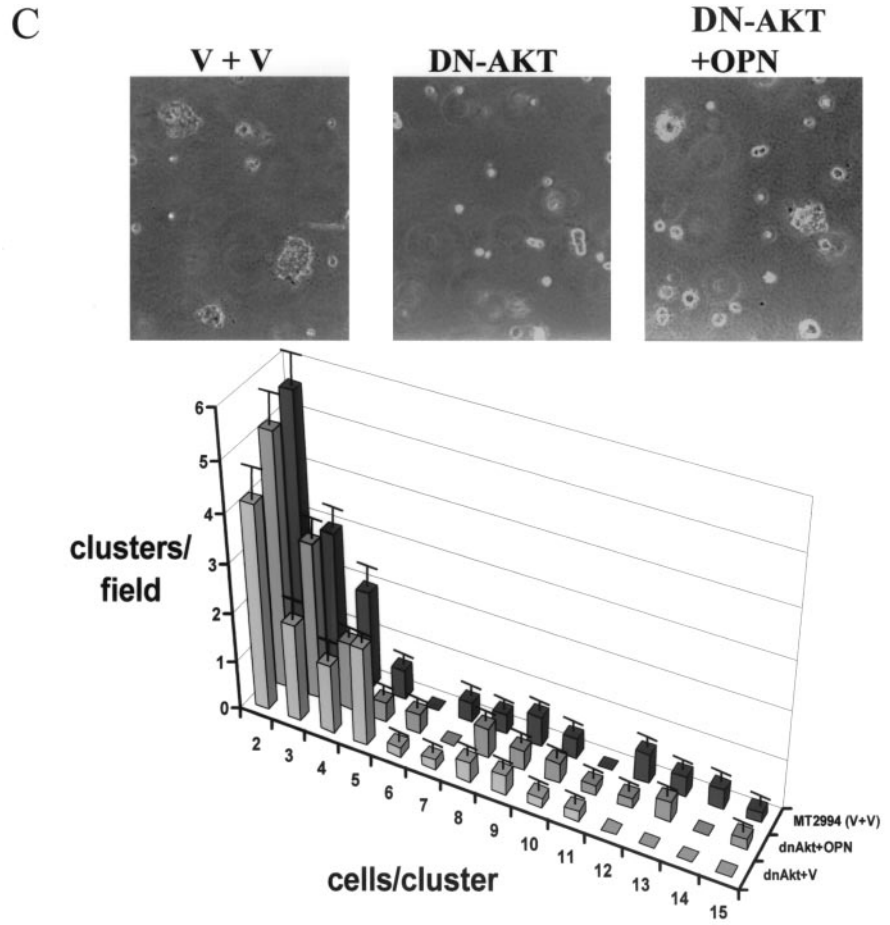

FIG. 6. Invasive growth depends on Akt kinase and osteopontin. (A) FSK-7 cells stably transfected with vector or with constitutively active Akt were plated in soft agar with repeated additions of either an antiosteopontin antibody or a control immunoglobulin. After 21 days, the frequency of clone formation and the clone size (numbers of cells per cluster) were enumerated in five random microscopic fields. The number of clusters per field is plotted against the number of cells per cluster for each cell line and treatment. ca-Akt, constitutively active Akt; IgG, immunoglobulin; OPN, osteopontin. (B) FSK-7 cells were transfected with either vector plus vector (V + V), constitutively active Akt plus vector, or constitutively active Akt plus antisense to osteopontin. Cells (5×10^5 per 60-mm-diameter dish) were grown in soft agar for 21 days. Micrographs were taken at a high magnification. Clone formation and clone size were enumerated in five random microscopic fields. (C) MT2994 cells transfected with either vector plus vector, dominant-negative Akt plus vector, or dominant-negative Akt plus osteopontin. CA-AKT, constitutively active Akt; dnAkt, dominant-negative Akt; V, vector; OPN, osteopontin; AS-OPN, antisense osteopontin. Error bars, standard errors. *, $P < 0.1$; **, $P < 0.05$; ***, $P < 0.01$.

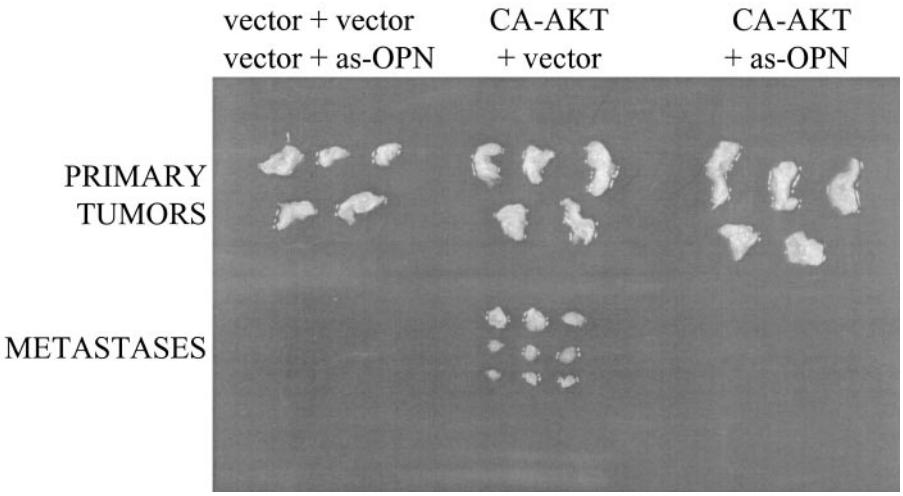

FIG. 7. In vivo growth and dissemination are mediated by Akt kinase and osteopontin. FSK-7 cells were doubly transduced, and 10^6 cells were injected orthotopically into the left inguinal mammary fat pads of BALB/c mice. One group of five mice received either FSK-7 cells transduced with vector plus vector or FSK-7 cells transduced with vector plus antisense osteopontin (as-OPN), five mice were injected with FSK-7 cells transduced with constitutionally activated Akt (CA-AKT) plus vector, and five mice were given FSK-7 cells transduced with constitutionally activated Akt plus antisense osteopontin. After 30 days, the mice were analyzed for tumor formation and metastasis. Primary tumors are shown at the top, and metastases detected during necropsy are shown at the bottom.

human breast carcinogenesis and could contribute to ligand-independent breast cancer cell growth (46). Here we describe a single molecular defect responsible for both growth dysregulation and induction of metastatic potential in breast cancer cells. It enhances our molecular insights into carcinogenesis and defines candidate targets for therapeutic intervention.

ACKNOWLEDGMENTS

This study was supported by National Institutes of Health research grant CA76176 and U.S. Army breast cancer grant BC011270 to G.F.W.

We are grateful to Joseph Jerry for kindly providing the cell lines. We thank Thomas Franke for generously sharing the Akt kinase constructs and David Denhardt for supplying the osteopontin reporter constructs.

REFERENCES

1. **Adler, B., G. F. Weber, and H. Cantor.** 1998. Activation of T-cells by superantigen: cytokine production but not apoptosis depends on MEK-1 activity. Eur. J. Immunol. **28:**3749–3754.
2. **Atkins, K. B., R. U. Simpson, and M. J. Somerman.** 1997. Stimulation of osteopontin mRNA expression in HL-60 cells is independent of differentiation. Arch. Biochem. Biophys. **343:**157–163.
3. **Barcellos-Hoff, M. H., and S. A. Ravani.** 2000. Irradiated mammary gland stroma promotes the expression of tumorigenic potential by unirradiated epithelial cells. Cancer Res. **60:**1254–1260.
4. **Barraclough, R., H. J. Chen, B. R. Davies, M. P. Davies, Y. Ke, B. H. Lloyd, A. Oates, and P. S. Rudland.** 1998. Use of DNA transfer in the induction of metastasis in experimental mammary systems. Biochem. Soc. Symp. **63:**273–294.
5. **Biswas, D. K., A. P. Cruz, E. Gansberger, and A. B. Pardee.** 2000. Epidermal growth factor-induced nuclear factor κB activation: a major pathway of cell-cycle progression in estrogen-receptor negative breast cancer cells. Proc. Natl. Acad. Sci. USA **97:**8542–8547.
6. **Brockhoff, G., P. Heiss, J. Schlegel, F. Hofstaedter, and R. Knuechel.** 2001. Epidermal growth factor receptor, c-erbB2 and c-erbB3 receptor interaction, and related cell cycle kinetics of SK-BR-3 and BT474 breast carcinoma cells. Cytometry **44:**338–348.
7. **Carles-Kinch, K., K. E. Kilpatrick, J. C. Stewart, and M. S. Kinch.** 2002. Antibody targeting of the EphA2 tyrosine kinase inhibits malignant cell behavior. Cancer Res. **62:**2840–2847.
8. **Chackalaparampil, I., A. Peri, M. Nemir, M. D. Mckee, P. H. Lin, B. B. Mukherjee, and A. B. Mukherjee.** 1996. Cells in vivo and in vitro from osteopetrotic mice homozygous for c-*src* disruption show suppression of synthesis of osteopontin, a multifunctional extracellular matrix protein. Oncogene **12:**1457–1467.
9. **Chambers, A. F., E. I. Behrend, S. M. Wilson, and D. T. Denhardt.** 1992. Induction of expression of osteopontin (OPN; secreted phosphoprotein) in metastatic, *ras*-transformed NIH 3T3 cells. Anticancer Res. **12:**43–48.
10. **Chambers, A. F., and A. B. Tuck.** 1993. Ras-responsive genes and tumor metastasis. Crit. Rev. Oncog. **4:**95–114.
11. **Chen, H., Y. Ke, A. J. Oates, R. Barraclough, and P. S. Rudland.** 1997. Isolation of and effector for metastasis-inducing DNAs from a human metastatic carcinoma cell line. Oncogene **14:**1581–1588.
12. **Cheng, H.-L., M. Steinway, C. L. Delaney, T. F. Franke, and E. L. Feldman.** 2000. IGF-I promotes Schwann cell motility and survival via action of Akt. Mol. Cell. Endocrinol. **170:**211–215.
13. **Craig, A. M., G. T. Bowden, A. F. Chambers, M. A. Spearman, A. H. Greenberg, J. A. Wright, M. McLeod, and D. T. Denhardt.** 1990. Secreted phosphoprotein mRNA is induced during multi-stage carcinogenesis in mouse skin and correlates with the metastatic potential of murine fibroblasts. Int. J. Cancer **46:**133–137.
14. **Craig, A. M., M. Nemir, B. B. Mukherjee, A. F. Chambers, and D. T. Denhardt.** 1988. Identification of the major phosphoprotein secreted by many rodent cell lines as 2ar/osteopontin: enhanced expression in H-ras-transformed 3T3 cells. Biochem. Biophys. Res. Commun. **157:**166–173.
15. **Denhardt, D. T., C. M. Giachelli, and S. R. Rittling.** 2001. Role of osteopontin in cellular signaling and toxicant injury. Annu. Rev. Pharmacol. Toxicol. **41:**723–749.
16. **Dimri, G. P., K. Ithana, M. Acosta, and J. Campisi.** 2000. Regulation of a senescence checkpoint response by the E2F1 transcription factor and $p14^{ARF}$ tumor suppressor. Mol. Cell. Biol. **20:**273–285.
17. **Dunn, S. E., J. V. Torres, J. S. Oh, D. M. Cykert, and J. C. Barrett.** 2001. Up-regulation of urokinase-type plasminogen activator by insulin-like growth factor-I depends upon phosphatidylinositol-3 kinase and mitogen-activated protein kinase kinase. Cancer Res. **61:**1367–1374.
18. **Eder, A. M., L. Dominguez, T. F. Franke, and J. D. Ashwell.** 1998. Phosphoinositide 3-kinase regulation of T cell receptor-mediated interleukin-2 gene expression in normal T cells. J. Biol. Chem. **273:**28025–28031.
19. **El-Tanani, M., R. Barraclough, M. C. Wilkinson, and P. S. Rudland.** 2001. Metastasis-inducing DNA regulates the expression of the osteopontin gene by binding the transcription factor Tcf-4. Cancer Res. **61:**5619–5629.
20. **El-Tanani, M. K., R. Barraclough, M. C. Wilkinson, and P. S. Rudland.** 2001. Regulatory region of metastasis-inducing DNA is the binding site for T cell factor-4. Oncogene **20:**1793–1797.
21. **Giap, A. Q., A. Tarnawski, N. T. Hoa, V. Akotia, and Y. Ma.** 2002. NSAID inhibition of RGM1 gastric monolayer wound re-epithelialization: comparison of selective Cox-2 versus non-selective Cox inhibitors. Life Sci. **70:**3029–3037.
22. **Gunthert, U., M. Hofmann, W. Rudy, S. Reber, M. Zoller, I. Haussmann, S. Matzku, A. Wenzel, H. Ponta, and P. Herrlich.** 1991. A new variant of glycoprotein CD44 confers metastatic potential to rat carcinoma cells. Cell **65:**13–24.
23. **Guo, X., Y. P. Zhang, D. A. Mitchell, D. T. Denhardt, and A. F. Chambers.** 1995. Identification of a ras-activated enhancer in the mouse osteopontin promoter and its interaction with a putative ETS-related transcription factor whose activity correlates with the metastatic potential of the cell. Mol. Cell. Biol. **15:**476–487.
24. **Hermanto, U., C. S. Zong, and L. H. Wang.** 2001. ErbB2-overexpressing human mammary carcinoma cells display an increased requirement for the phosphatidylinositol 3-kinase signaling pathway in anchorage-independent growth. Oncogene **20:**7551–7562.
25. **James, N. H., J. Ashby, and R. A. Roberts.** 1995. Enhanced hepatocyte colony growth in soft agar after in vivo treatment with a genotoxic carcinogen: a potential assay for hepatocarcinogens? Cancer Lett. **93:**121–128.
26. **Jerry, D. J., M. A. Ozbun, F. S. Kittrell, D. P. Lane, D. Medina, and J. S. Butel.** 1993. Mutations in *p53* are frequent in the preneoplastic stage of mouse mammary tumor development. Cancer Res. **53:**3374–3381.
27. **Katz, R. W., S. Y. Teng, S. Thomas, and R. Landesberg.** 2002. Paracrine activation of extracellular signal-regulated kinase in a simple in vitro model of wounded osteoblasts. Bone **31:**288–295.
28. **Kitaura, J., K. Asai, M. Maeda-Yamamoto, Y. Kawakami, U. Kikkawa, and T. Kawakami.** 2000. Akt-dependent cytokine production in mast cells. J. Exp. Med. **192:**729–740.
29. **Kittrell, F. S., C. J. Oborn, and D. Medina.** 1992. Development of mammary preneoplasias *in vivo* from mouse mammary epithelial cell lines *in vitro*. Cancer Res. **52:**1924–1932.
30. **Kuppumbatti, Y. S., B. Rexer, S. Nakajo, K. Nakaya, and R. Mira-y-Lopez.** 2001. CRBP suppresses breast cancer cell survival and anchorage-independent growth. Oncogene **20:**7413–7419.
31. **Lenferink, A. E., D. Busse, W. M. Flanagan, F. M. Yakes, and C. L. Arteaga.** 2001. ErbB2/neu kinase modulates cellular $p27^{Kip1}$ and cyclin D1 through multiple signaling pathways. Cancer Res. **61:**6583–6591.
32. **Li, W., J. Zhang, L. Flechner, T. Hyun, A. Yam, T. F. Franke, and J. H. Pierce.** 1999. Protein kinase C-α overexpression stimulates Akt activity and suppresses apoptosis induced by interleukin 3 withdrawal. Oncogene **18:**6564–6572.
33. **Lim, S. J., G. Lopez-Berestein, M. C. Hung, R. Lupu, and A. M. Tari.** 2000. Grb2 downregulation leads to Akt inactivation in heregulin-stimulated and ErbB2-overexpressing breast cancer cells. Oncogene **19:**6271–6276.
34. **Malyankar, U. M., M. Almeida, R. J. Johnson, R. H. Pichler, and C. M. Giachelli.** 1997. Osteopontin regulation in cultured rat renal epithelial cells. Kidney Int. **51:**1766–1773.
35. **Moasser, M. M., A. Basso, S. D. Averbuch, and N. Rosen.** 2001. The tyrosine kinase inhibitor ZD1839 ("Iressa") inhibits HER2-driven signaling and suppresses the growth of HER2-overexpressing tumor cells. Cancer Res. **61:**7184–7188.
36. **Nakanishi, K., M. Sakamoto, J. Yasuda, M. Takamura, N. Fujita, T. Tsuruo, S. Todo, and S. Hirohashi.** 2002. Critical involvement of the phosphatidylinositol 3-kinase/Akt pathway in anchorage-independent growth and hematogeneous intrahepatic metastasis of liver cancer. Cancer Res. **62:**2971–2975.
37. **Nose, K., H. Saito, and T. Kuroki.** 1990. Isolation of a gene sequence induced later by tumor-promoting 12-*O*-tetradecanoylphorbol-13-acetate in mouse osteoblastic cells (MC3T3-E1) and expressed constitutively in ras-transformed cells. Cell Growth Differ. **1:**511–518.
38. **Oates, A. J., R. Barraclough, and P. S. Rudland.** 1996. The identification of osteopontin as a metastasis-related gene product in a rodent mammary tumour model. Oncogene **13:**97–104.
39. **Ozbun, M. A., D. J. Jerry, F. S. Kittrell, D. Medina, and J. S. Butel.** 1993. p53 mutations selected *in vivo* when mouse mammary epithelial cells form hyperplastic outgrowths are not necessary for establishment of mammary cell lines *in vitro*. Cancer Res. **53:**1646–1652.
40. **Park, B.-K., X. Zeng, and R. Glazer.** 2001. Akt1 induces extracellular matrix invasion and matrix metalloproteinase-2 activity in mouse mammary epithelial cells. Cancer Res. **61:**7647–7653.
41. **Pianetti, S., M. Arsura, R. Romieu-Mourez, R. J. Coffey, and G. E. Sonenshein.** 2001. Her-2/neu overexpression induces NF-κB via a PI3-kinase/Akt

pathway involving calpain-mediated degradation of IκB-α that can be inhibited by the tumor suppressor PTEN. Oncogene **20:**1287–1299.
42. **Rudland, P. S., A. Platt-Higgins, M. El-Tanani, S. De Silva Rudland, R. Barraclough, J. H. Winstanley, R. Howitt, and C. R. West.** 2002. Prognostic significance of the metastasis-associated protein osteopontin in human breast cancer. Cancer Res. **62:**3417–3427.
43. **Ryo, A., Y. C. Liou, G. Wulf, M. Nakamura, S. W. Lee, and K. P. Lu.** 2002. PIN1 is an E2F target gene essential for Neu/Ras-induced transformation of mammary epithelial cells. Mol. Cell. Biol. **22:**5281–5295.
44. **Seiter, S., R. Arch, S. Reber, D. Komitowski, M. Hofmann, H. Ponta, P. Herrlich, S. Matzku, and M. Zoller.** 1993. Prevention of tumor metastasis formation by anti-variant CD44. J. Exp. Med. **177:**443–455.
45. **Singhal, H., D. S. Bautista, K. S. Tonkin, F. P. O'Malley, A. B. Tuck, A. F. Chambers, and J. F. Harris.** 1997. Elevated plasma osteopontin in metastatic breast cancer associated with increased tumor burden and decreased survival. Clin. Cancer Res. **3:**605–611.
46. **Sun, M., J. E. Paciga, R. I. Feldman, A. Yuan, D. Coppola, Y. Y. Lu, S. A. Shelley, S. V. Nicosia, and J. Q. Cheng.** 2001. Phosphatidylinositol-3-OH kinase (PI3K)/AKT2, activated in breast cancer, regulates and is induced by estrogen receptor α (ERα) via interaction between ERα and PI3K. Cancer Res. **61:**5985–5991.
47. **Sung, V., C. Gilles, A. Murray, R. Clarke, A. D. Aaron, N. Azumi, and E. W. Thompson.** 1998. The LCC15-MB human breast cancer cell line expresses osteopontin and exhibits an invasive and metastatic phenotype. Exp. Cell Res. **241:**273–284.
48. **Tanno, S., S. Tanno, Y. Mitsuuchi, A. Altomare, G.-H. Xiao, and J. R. Testa.** 2001. AKT activation up-regulates insulin-like growth factor I receptor expression and promotes invasiveness of human pancreatic cancer cells. Cancer Res. **61:**589–593.
49. **Tsai, E. M., S. C. Wang, J. N. Lee, and M. C. Hung.** 2001. Akt activation by estrogen in estrogen receptor-negative breast cancer cells. Cancer Res. **61:**8390–8392.
50. **Tuck, A. B., D. M. Arsenault, F. P. O'Malley, C. Hota, M. C. Ling, S. M. Wilson, and A. F. Chambers.** 1999. Osteopontin induces increased invasiveness and plasminogen activator expression of human mammary epithelial cells. Oncogene **18:**4237–4246.
51. **Urquidi, V., D. Sloan, K. Kawai, D. Agarwal, A. C. Woodman, D. Tarin, and S. Goodison.** 2002. Contrasting expression of thrombospondin-1 and osteopontin correlates with absence or presence of metastatic phenotype in an isogenic model of spontaneous human breast cancer metastasis. Clin. Cancer Res. **8:**61–74.
52. **Weber, G. F.** 2001. The metastasis gene osteopontin: a candidate target for cancer therapy. Biochim. Biophys. Acta **1552:**61–85.
53. **Weber, G. F., and S. Ashkar.** 2000. Stress response genes—the genes that make cancer metastasize. J. Mol. Med. **78:**404–408.
54. **Weber, G. F., R. Bronson, J. Ilagan, H. Cantor, R. Schmitz, and T. W. Mak.** 2002. Absence of CD44 prevents sarcoma metastasis. Cancer Res. **62:**2281–2286.
55. **Zhang, R. D., I. J. Fidler, and J. E. Price.** 1991. Relative malignant potential of human breast carcinoma cell lines established from pleural effusions and a brain metastasis. Invasion Metastasis **11:**204–215.
56. **Zhou, B. P., Y. Liao, W. Xia, B. Spohn, M. H. Lee, and M. C. Hung.** 2001. Cytoplasmic localization of p21Cip1/WAF1 by Akt-induced phosphorylation in HER-2/neu-overexpressing cells. Nat. Cell Biol. **3:**245–252.

Oncogene (2005), 1–11

www.nature.com/onc

ORIGINAL ARTICLE

An osteopontin splice variant induces anchorage independence in human breast cancer cells

B He[1,3], M Mirza[2,3] and GF Weber[1,2]

[1]*Molecular Oncology Research Institute, New England Medical Center, Boston, MA, USA and* [2]*University of Cincinnati Medical Center, College of Pharmacy, Cincinnati, OH, USA*

In malignant tumors, metastasis genes are typically deregulated by aberrant expression or splicing. Osteopontin is expressed at high levels by various cancers and contributes importantly to their invasive potential. In contrast, osteopontin derived from host cells induces cellular immunity and could bolster antitumor protection by cytotoxic T lymphocytes. Here we show that breast cancer cells express multiple splice variants of osteopontin. According to RT–PCR analysis of human breast tissue specimens, the splice variant osteopontin-c is a highly specific marker for transformed cells, which is not expressed in their surrounding normal tissue. The full-length form of osteopontin aggregates in the presence of physiologic amounts of calcium and, in this state, leads to enhanced cell adhesion. Ostensibly, this effect is inhibitory for tumor cell dissemination. The shortest splice variant, osteopontin-c, does not aggregate in the presence of calcium and enhances clone formation in soft agar. According to microarray analysis, osteopontin-c induces the expression of oxidoreductases, consistent with protection from anoikis during anchorage-independent growth. These studies define a third functional domain of osteopontin, beside the C-terminal CD44-binding site and the central integrin-binding site. They also provide evidence for a bifunctional character of osteopontin, with the soluble form supporting invasiveness and the aggregated form promoting adhesion.
Oncogene advance online publication, 14 November 2005; doi:10.1038/sj.onc.1209248

Keywords: breast cancer; alternative splicing; cell adhesion; metastasis; soft agar

Introduction

The genetic basis of cancer dissemination has been subject to intense debate. We have identified metastasis genes as stress response genes, which in cancer are deregulated on the levels of aberrant expression and splicing (Weber and Ashkar, 2000a, b). The cytokine osteopontin (OPN) is frequently secreted by cancer cells and plays important roles in their ability to metastasize (Sung *et al*., 1998; Urquidi *et al*., 2002; El-Tanani *et al*., 2001a, b). Its expression is necessary and may be sufficient for invasiveness by breast tumors (Tuck *et al*., 1999; Zhang *et al*., 2003). Multiple metastatic breast cancer cell lines express osteopontin, and transfection of the osteopontin gene into benign tumorigenic human breast epithelial cell lines conveys invasive behavior (Chen *et al*., 1997; Barraclough *et al*., 1998). Increasing the expression of osteopontin or transfection of osteopontin-encoding cDNA into a previously benign cell line is sufficient to produce a metastatic phenotype in a rat mammary model (Oates *et al*., 1996). Furthermore, high levels of osteopontin in the plasma or in the tumor are an adverse prognostic factor in breast carcinoma (Singhal *et al*., 1997; Rudland *et al*., 2002). Osteopontin binds to the metastasis-associated cell surface receptors integrin $\alpha_V\beta_3$ and CD44v3–6 and mediates cell migration. Osteopontin-induced chemotaxis is conveyed through the binding of a C-terminal domain to a CD44 splice variant (Weber *et al*., 1996). Cells can also move up a gradient of immobilized ligand. This cell crawling may occur on vessel walls or in the interstitium and is referred to as haptotaxis. Haptotaxis toward osteopontin is mediated through ligation of the integrin $\alpha_V\beta_3$ by a N-terminal osteopontin domain. Integrin engagement depends not only on the RGD motif, but also on the phosphorylation of specific osteopontin sites (Weber *et al*., 2002). Of note, the physiologic or patho-physiologic roles of the far N-terminal osteopontin domains (including exons 4 and 5) have not yet been defined.

The immune system may protect from tumorigenesis. The cellular arm, activating cytotoxic T lymphocytes and natural killer cells as effectors, is considered to be a critical part of this immune surveillance. The cytokine osteopontin is secreted by activated helper T lymphocytes and is essential for the induction of cellular immune responses (Ashkar *et al*., 2000; O'Regan *et al*., 2000; Adler *et al*., 2001). Osteopontin induces the secretion of IL-12 from macrophages, a cytokine that is effective in activating antitumor immunity (Chen *et al*., 1996; Zitvogel *et al*., 1996). Host osteopontin also

Correspondence: Dr GF Weber, University of Cincinnati Medical Center, College of Pharmacy, 3225 Eden Avenue, Cincinnati, OH 45267-0004, USA.
E-mail: georg.weber@uc.edu
[3]These authors contributed equally to this work.
Received 8 September 2005; revised 12 October 2005; accepted 12 October 2005

acts as a macrophage chemoattractant and thus contributes to the antitumor host defense, whereas tumor osteopontin inhibits macrophage function (Crawford *et al*., 1998). The structural basis for the potential of host-derived osteopontin to contribute to suppressing tumor formation, whereas osteopontin secreted by transformed cells enhances their metastatic propensity, has not been elucidated.

Heterogeneity of osteopontin derived from various cellular sources has been described previously, but the underlying biochemical processes are incompletely understood. By Western blotting and in a set of sandwich ELISA setups, characterized by the use of various antibody combinations, tumor-derived osteopontin was differentially detected (Rittling and Feng, 1998; Kon *et al*., 2000). Osteopontin forms of distinct sizes, according to SDS–PAGE, are secreted by tumor cells and their nontransformed counterparts. Specifically, cancer cells may secrete a splice variant that has a deletion in its N-terminal portion (Kiefer *et al*., 1989). As a case in point, an osteosarcoma secreted a smaller form of osteopontin than the predominant product generated by nontransformed bone cells. The secretion of the smaller form correlated with anchorage independence (Chackalaparampil *et al*., 1985; Kasugai *et al*., 1991). This may reflect a loss of adhesion to osteopontin because, in contrast to host osteopontin, tumor-derived osteopontin fails to associate with the extracellular matrix and remains soluble (Rittling *et al*., 2002).

The existence in humans of two osteopontin splice variants with deletions of exon 4 (referred to as osteopontin-c) or 5 (called osteopontin-b) (Figure 1a) has been described (Young *et al*., 1990) and has been observed to be expressed in glioma cells (Saitoh *et al*., 1995). Differences in the physiologic roles among these variants have not been studied. Here we test the possibility that splice variants of osteopontin may be expressed selectively in malignant tumors and facilitate their dissemination. The functional alterations associated with the alternatively spliced exons may account for the observed differences between host and tumor osteopontin.

Results

Multiple osteopontin forms are expressed by breast cancer cells

We analysed osteopontin gene expression in various breast tumor cells by RT–PCR using primers that span an upstream region covering exons 2–6. To eliminate skewing of the results by activation of the cells through growth factors in the medium, we used serum-free conditions. The malignant breast cancer cell lines MDA-MB-435 and MDA-MB-231 express three distinct RNA messages of osteopontin. MCF-7 cells are noninvasive and do not contain measurable osteopontin RNA levels (Figure 1b). The two smaller osteopontin transcript bands selectively expressed in malignant cells were identified by cloning and sequencing as splice variants missing the third or fourth translated exons (exons 4 or 5, because exon 1 is untranslated (Behrend *et al*., 1993)). Other invasive cell lines tested, including cancers of diverse tissue origin, express multiple osteopontin messages (Hela, SAOS-2, 21MT1, 21MT2), while all noninvasive cell lines tested (ZR-75-1, 21NT, LnCAP) express no osteopontin or low levels of osteopontin-a without splice variants (data not shown). The identified transcripts correspond to the sequences of 'osteopontin-a,' 'osteopontin-b' and 'osteopontin-c,' which are listed in GenBank (Accession numbers D28759, D28760, and D28761) but have not been thoroughly studied. Published reports on the expression or function of the splice variants are limited to the observation of three types of osteopontin RNA messages in human gliomas (Saitoh *et al*., 1995) and to the existence of a splice variant that has a deletion in its N-terminal portion (Kiefer *et al*., 1989). The secretion of multiple osteopontin forms by

Figure 1 Expression of osteopontin RNA in breast tumor cell lines. (**a**) Structural characteristics of the osteopontin gene product. Top: The gene has six translated exons. The sequences for splice variants of exons 4 (osteopontin-c) or 5 (osteopontin-b) are listed in Genbank. Middle: Two main domains on the protein are separated by a protease-sensitive site, a N-terminal fragment encompasses the integrin-binding domains, while the CD44v-binding domain lies on the C-terminal part of the molecule. Bottom: The integrin-binding site covers the sequence GRGDS. The smallest integrin $\alpha_V\beta_3$-binding peptide identified by us starts at AA71 (Weber *et al*., 2002). Binding to β_1-containing integrins occurs through the noncanonical sequence SVVYGLR (Yokosaki *et al*., 1999), unless the β_1 chain is paired with α_4, in which case the binding site ranges from AA131 to AA144 (Bayless *et al*., 1998). We have found the CD44v3–6-binding site to cover the region from AA169 to AA220 (Ashkar *et al*., 2000 and Ashkar/Weber unpublished results). Heparin bridges between osteopontin and CD44v3 may be formed via the heparin-binding sites on AA170 and 300. Note that AA1-70 are not known to be involved in receptor ligation, their function has not been defined. The bases of the coding sequence and the corresponding amino acids are numbered such that the start site, or initiating methionine is 1. The scheme is not drawn to scale. (**b**) The cells were plated at 1×10^5/well in 24-well plates and allowed to adhere for 7 h before starvation in growth factor- and serum-deprived medium. Total RNA was extracted, reverse transcribed with oligo-dT and PCR was performed with primers that span the region from base pairs 50 to 246 with the primers 5′-tac cag tta aac agg ctg att c-3′ and 5′-cca tat cat cca tgt ggt ca-3′. PCR of GAPDH was used as a control for the amount of template present. OPN = osteopontin; GAPDH = glyceraldehyde 3-phosphate dehydrogenase. The slowest migrating band (no arrow) seen in MDA-MB-435 cells was often present in the no-template control sample and is deemed to be nonspecific. MCF-7 cells are noninvasive while MDA-MB-435 and MDA-MB-231 are metastatic. (**c**) Western blotting to detect secreted osteopontin in cell culture supernatant. ZR75-1 is noninvasive. Supernatant from MCF-7 cells transfected with osteopontin-c was loaded as a positive control. The lower panel shows a Western blot at low exposure to demonstrate the separation of three bands in the MDA-MB-435 supernatants. (**d**) The expression of osteopontin-a and osteopontin-c in human breast tissue specimens was assessed by RT–PCR (with amplification of GAPDH controlling for template integrity and abundance). According to the intensity of the resulting band on agarose gel, the expression levels were rated as high, low, or absent. Indicated are the numbers of specimens identified in each group. The panel to the right shows the RT–PCR results for a representative invasive DCIS (ductal carcinoma *in situ*) sample (T) and its surrounding normal tissue (N), M = size markers.

the invasive breast cancer cell line MDA-MB-435, but not by the noninvasive breast tumors MCF-7 and ZR-75-1 was confirmed by Western blotting (Figure 1c).

Through the tissue repository at the University of Cincinnati Medical Center, we obtained breast tumor specimens, surrounding nontransformed tissue, and normal breast tissue (derived from reduction mammoplasty). We performed RT–PCR with pairs of primers that are specific for the splice variants osteopontin-a or -c (amplification of GAPDH served as a control for

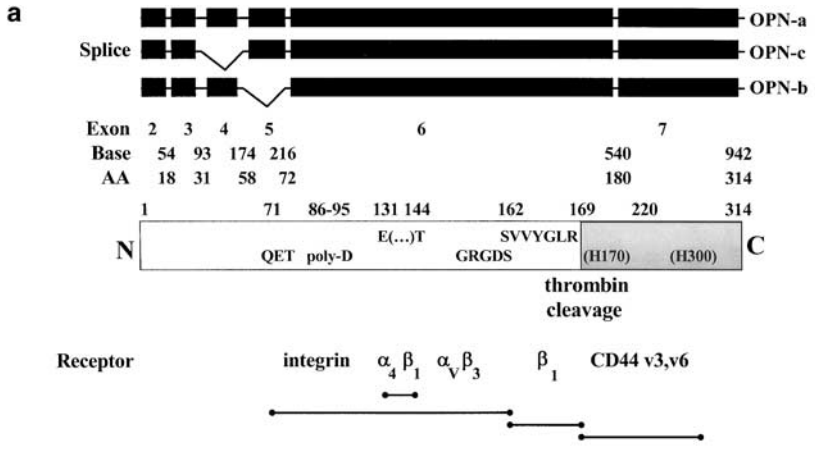

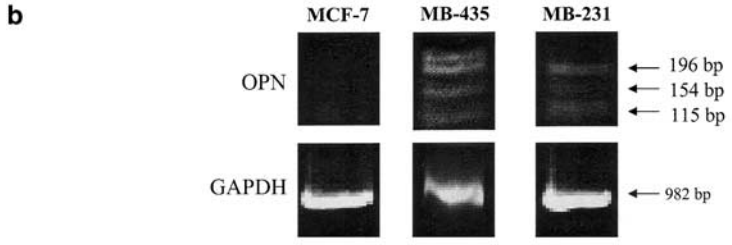

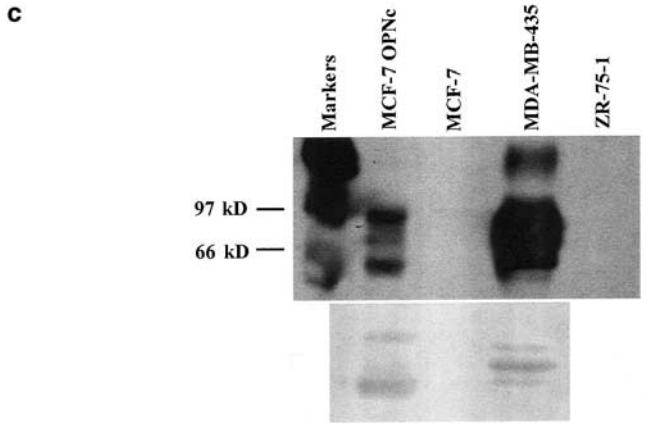

d

	breast cancer	surrounding normal	invasive DCIS	surrounding normal	normal
OPNa					
high	3	0	5	0	1
low	0	1	0	3	5
absent	1	1	0	0	5
OPNc					
high	3	0	3	0	0
low	0	0	2	0	0
absent	1	2	0	3	11

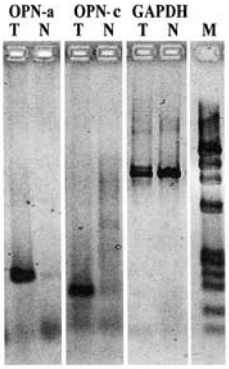

abundance and integrity of the cDNA, amplification without a template confirmed the absence of aerosol contamination). Three of four breast carcinomas expressed high levels of osteopontin-c. For two of them, surrounding tissue was available, one of which expressed low levels of osteopontin-a, but neither expressed detectable levels of osteopontin-c. We also studied five invasive ductal carcinomas. All expressed osteopontin-a and -c messages. While the surrounding tissue, available from three patients, had low amounts of osteopontin-a, none expressed osteopontin-c. The expression levels of osteopontin-a varied in 11 specimens of normal breasts. This may reflect the production of unspliced osteopontin, which is physiologically secreted in milk, by breast cells depending on the stages of the estrous cycle. Osteopontin-c transcripts were never detected in the normal tissue samples (Figure 1d). These results suggest that osteopontin splicing is specific to tumor cells.

Osteopontin-c facilitates soft agar colony formation more than osteopontin-a

We stably transduced full-length osteopontin (variant a) and splice variant c into MCF-7 cells, which do not express endogenous osteopontin (Figure 2a and b). After incubation of the cells for 14 h in serum-free medium, abundant amounts of osteopontin were secreted into the supernatants of the transfected cells, but not the vector controls. Consistent with previous observations (Tuck *et al*., 1999), a second, slower migrating band was observed, possibly reflecting phosphorylation or glycosylation. The smaller band could result from thrombin cleavage of this modified form. Overexpression of osteopontin was also seen in the cell lysates.

Because we had previously found osteopontin to facilitate clone formation in soft agar (Zhang *et al*., 2003), we tested whether the transfection of osteopontin-a or -c changed the phenotype of MCF-7 cells in this assay. In fact, osteopontin-c facilitated soft agar clone formation and the clones formed after 7 days show distinct protrusions, which are absent from osteopontin-a-transfected cells or vector controls and which we believe to be indicative of the rapid expansion of the clones within the agar (Figure 3a and b). These changes were directly dependent on the osteopontin protein because the addition of anti-osteopontin antibody, but not control immunoglobulin, to the cultures every other day with the exchange of medium suppressed the formation of clones by the transfected MCF-7 cells. In contrast, the antibody had no effect on the clones formed by vector-transfected MCF-7 cells (Figure 3c). The clone sizes of osteopontin-a-transfected MCF-7 cells were moderately, but statistically significantly larger than the vector control, and osteopontin-c-transfected cells formed significantly larger colonies than osteopontin-a transfectants (Figure 3d). Similar results were obtained with additional clones (MCF-7 OPNa1, MCF-7 OPNc16).

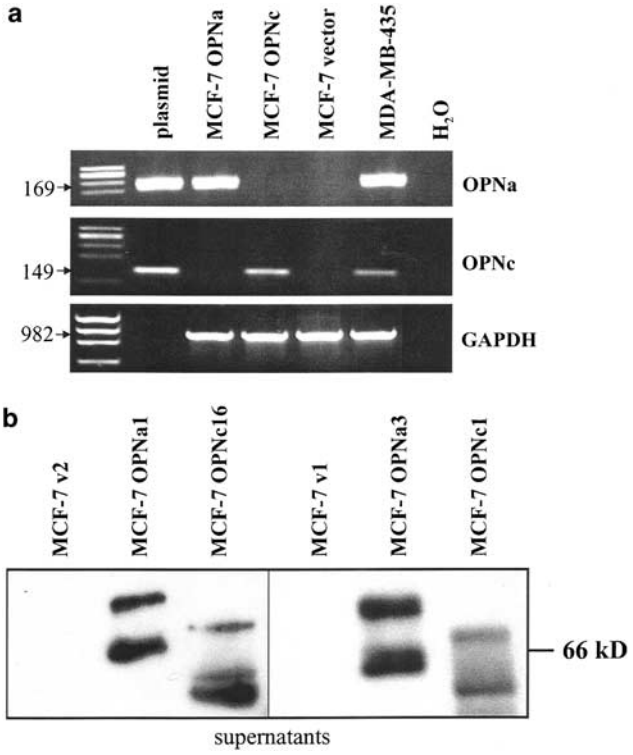

Figure 2 Stable expression of osteopontin splice variants in MCF-7 breast tumor cells. Osteopontin splice variants -a and -c were stably expressed in MCF-7 breast tumor cells, using stable transfection of the vector as a control. (**a**) RNA expression according to RT–PCR with primers specific for the splice variants osteopontin-a or -c. The housekeeping gene GAPDH served as a positive control. The markers are HaeIII fragments of ΦX174 RF DNA. (**b**) Clones were selected (indicated by numbers) and starved in serum-free medium for 14 h. The osteopontin expression levels were measured by Western blotting on supernatants (40 μl/lane). OPN = osteopontin. Please note that the detection of two bands on Western blot after transfection has been observed before. It may reflect post-translational modifications. Secondary antibody alone did not produce any signal (not shown). Additional stably expressing clones were selected and used in confirmatory experiments.

Neither osteopontin-c nor -a alters cell cycle progression

To account for the changes in soft agar growth characteristics, we first asked whether the growth rates of the osteopontin-expressing MCF-7 transfectants were altered as compared to a vector-transfected MCF-7 clone. Consistent with our earlier results, which had indicated that osteopontin expression affects motility but not cell growth (Zhang *et al*., 2003), there were no differences in cell numbers among MCF-7 vector, MCF-7 osteopontin-a, and MCF-7 osteopontin-c over 6 days of analysis (Figure 4a). Confirmatory experiments with additional stably transfected clones (MCF-7 v2, MCF-7 OPNa2, and MCF-7 OPNc16) yielded similar results.

Osteopontin-a, but not osteopontin-c supports calcium-dependent cell adhesion

As different growth rates did not account for the distinct phenotypes generated by osteopontin-a and -c in soft

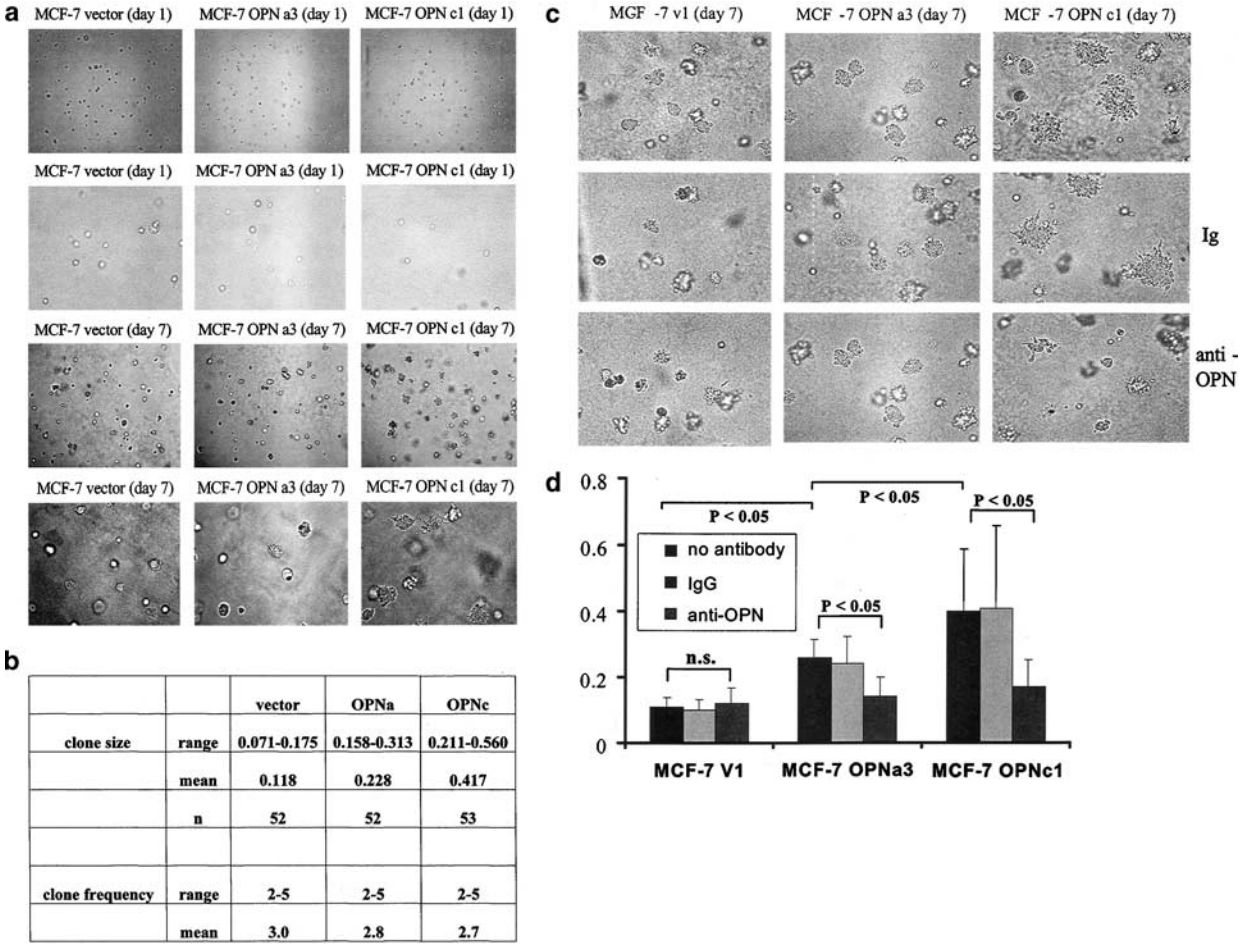

b

		vector	OPNa	OPNc
clone size	range	0.071-0.175	0.158-0.313	0.211-0.560
	mean	0.118	0.228	0.417
	n	52	52	53
clone frequency	range	2-5	2-5	2-5
	mean	3.0	2.8	2.7

Figure 3 Expression of the osteopontin splice variant-c enhances the colony formation in soft agar more than osteopontin-a. Transfected MCF-7 cells were plated in triplicates with a top layer of 0.3% agar and a bottom layer of 0.5% agar. Every other day, 0.4 ml of medium was supplemented and the plates were examined microscopically for growth. (**a**) Microscopic pictures were taken on days 1 (top panels) and 7 (bottom panels) after plating at low magnification (to show clone frequency) and at large magnification (to show clone size and shape). Protrusions from the clones formed are visible in MCF-7 OPNc1, but not in the MCF-7 cells transfected with osteopontin-a (MCF-7 OPNa3) or in the vector control (MCF-7 v1). (**b**) The combined data from three experiments were evaluated to determine the average clone size (relative units) and clone frequency, formed by MCF-7 cells transfected with vector, osteopontin-a, or osteopontin-c. 5 fields per plate were photographed and all clones in focus were measured. The table shows the mean and range of all measured clones (indicated as n). The differences among the groups in clone size, but not in clone frequency, were statistically significant according to the *t*-test. (**c**) Soft agar colony formation by transfected MCF-7 cells was evaluated in the absence of antibody (top panel) or with addition every other day of anti-osteopontin antibody at 0.5 μg/ml in 0.3 ml medium (bottom panel) or rabbit IgG (Sigma) as immunoglobulin control (middle panel). (**d**) The average clone size was quantitated by measuring the area of all focused colonies in five randomly chosen high-powered fields using image analysis software. The data represent mean $\pm$ s.d. The data sets were analysed for statistically significant differences by the *U*-test (Wilcoxon, Mann, and Whitney) and the *t*-test. The clone sizes for MCF-7 OPN-a and MCF-7 OPN-c are statistically significantly different from the clone sizes of MCF-7 vector and from one another. OPN = osteopontin.

agar, we set out to analyse MCF-7 cell adhesion as a factor that regulates anchorage independence. We found that GST-OPNa but not GST-OPNc had a tendency to aggregate in the presence of physiologic concentrations of calcium. The same phenomenon occurred with serum-free supernatants from the transfected MCF-7 cells (Figure 4b and c). Chelation with EDTA could prevent this phenomenon and magnesium, another divalent cation, could not substitute for calcium (Figure 4d). MCF-7 cells adhered to and spread dose dependently on increasing amounts of purified recombinant GST-OPN (Figure 4e and f). When plated with increasing amounts of calcium, the adhesion to GST-OPNa, but not to GST-OPNb or GST-OPNc, became stronger (Figure 4g).

Osteopontin influences the gene expression profile in soft agar

To further characterize the molecular basis for the enhancement of soft agar colony formation by osteopontin-c (increased clone size after 7 days, see Figure 3), we extracted the cellular RNA after 7 days of growth in soft agar and performed microarray analysis comparing MCF-7 OPNc16 to MCF-7 OPNa1 and to MCF-7 v1. In all, 525 genes were significantly differentially

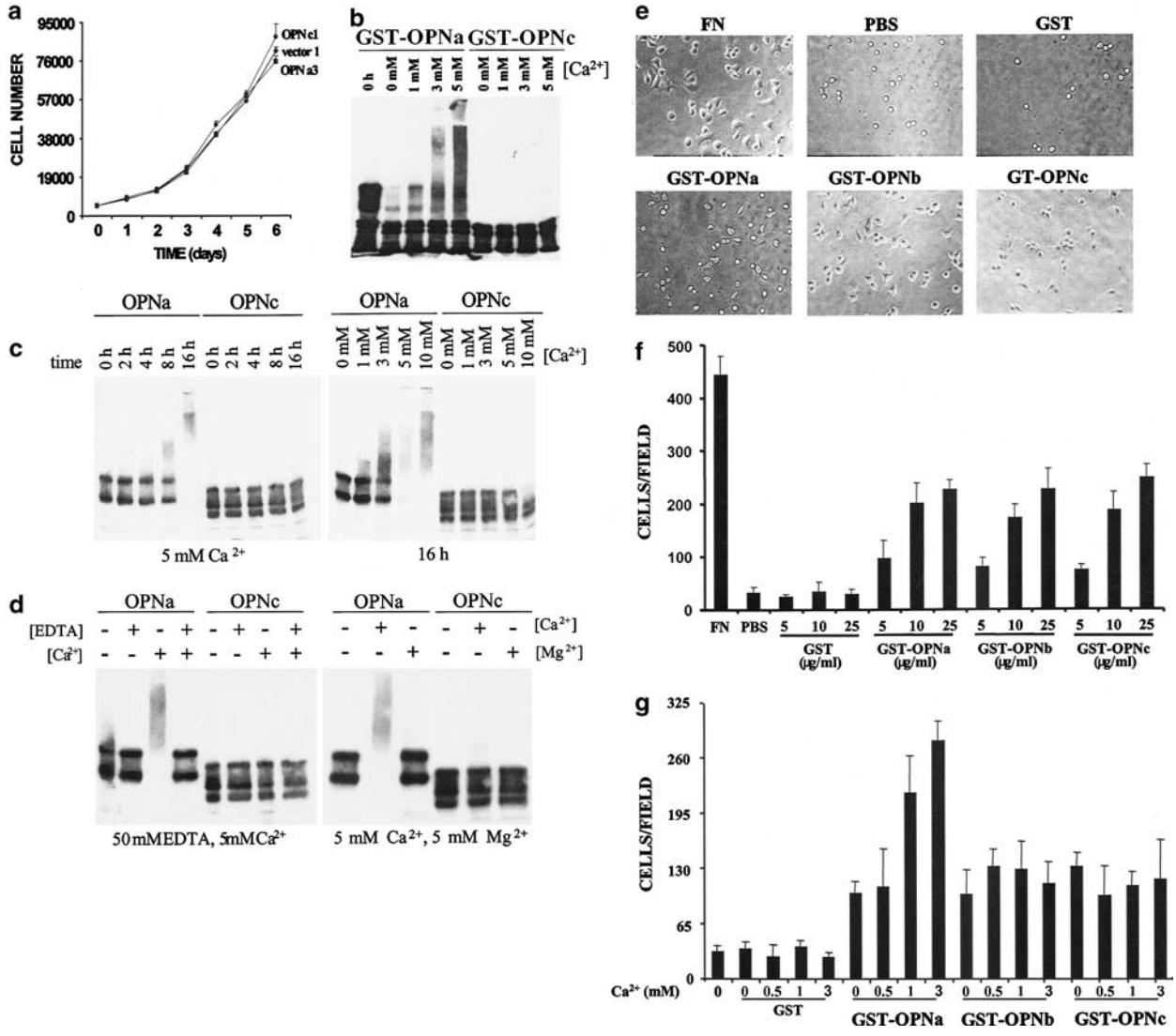

Figure 4 Osteopontin-c does not stimulate growth, but alters cell adhesion. (**a**) The expression of osteopontin splice variants does not affect the growth rate of MCF-7 cells. Stably transfected cells were plated at 5000 cells/well (24-well plate) on day 0. On every consecutive day, five wells per cell line were harvested and the total number of cells was counted in a Coulter Counter. Wilcoxon's test and *t*-test did not indicate statistically significant differences among the data sets. (**b**) Purified bacterial recombinant GST-OPNa aggregates in the presence of calcium, while GST-OPNc does not. Aggregation was assessed after 16 h at increasing concentrations of calcium. Consecutively denaturing, nonreducing SDS–PAGE and Western blotting for osteopontin was performed. (**c**) Osteopontin-a, but not osteopontin-c, aggregates in the presence of calcium. The supernatants from MCF-7 cells transfected with osteopontin-a or -c were incubated for increasing time periods at 5 mM calcium (left panel) or with increasing amounts of calcium for 16 h (right panel). (**d**) The need for calcium for osteopontin-a aggregation was assessed by reversal with 50 mM EDTA (left panel) or substitution with 5 mM magnesium (right panel). (**e** and **f**) Adhesion of MCF-7 cells to osteopontin splice variants. The wells of a 96-well plate were coated with GST-OPNs overnight. MCF-7 cells were allowed to adhere for 2 h at 37°C. (**e**) Microscopic pictures of the adhered cells after washing of the wells reflect cell spreading on plastic coated with fibronectin (FN) or GST-OPN, but not in the PBS control or in the well coated with GST. (**f**) Enumeration of cells adhered to wells coated with increasing amounts of GST-OPN. Fibronectin (FN) served as positive control and PBS as negative control. (**g**) Adhesion of MCF-7 cells to 10 μg/ml of purified GST-OPN fusion proteins, after coating of the wells in the presence of increasing amounts of calcium (0–3 mM).

Figure 5 Alterations in gene expression profiles induced by osteopontin-c and -a in soft agar. Cellular RNA was extracted from soft agar after 7 days, and subjected to linear amplification, cDNA synthesis and dye labeling for microarray analysis of MCF-7 OPNc compared to MCF-7 vector, MCF-7 OPNc compared to MCF-7 OPNa, and MCF-7 OPNa compared to vector. (**a**) Genes significantly altered (probability of error <0.005) by osteopontin-c as compared to vector according to EASE analysis. The Genbank accession numbers in italic are also detected as altered in the EASE analysis of osteopontin-c versus osteopontin-a. (**b**) Fold differences in expression within the groups of genes identified as significant in the EASE analysis for osteopontin-c versus vector (filled bars), osteopontin-c versus -a (gray bars), and osteopontin-a versus vector (open bars). The panels to the right indicate the *P*-values for significantly different expression of the individual genes (A-V = comparison of OPNa to vector, C-A = comparison of OPNc to OPNa, C-V = comparison of OPNc to vector).

a

Gene Category	List Hits	Population Hits	Probability	Benjamini FDR	Genbank
oxidoreductase activity	33	508	5.29×10^{-4}	4.01×10^{-2}	*AF258341*; AK002110; AK026717; BC014191; *BC015041*; NM_000159; NM_000302; NM_000689; NM_000786; *NM_000903*; NM_001360; NM_001513; NM_002085; NM_002134; *NM_002495*; NM_002631; NM_003142; NM_003273; NM_003366; NM_004551; NM_004718; NM_005002; *NM_005005*; NM_005125; NM_006440; NM_007103; NM_015380; NM_016011; NM_016527; *NM_016593*; NM_017547; *NM_024407*; *NM_025159*
cation transporter activity	15	195	3.88×10^{-3}	2.20×10^{-1}	AB032996; AB051548; AK002110; NM_001687; NM_001693; *NM_002495*; NM_003366; *NM_003945*; NM_004551; NM_004718; NM_005002; *NM_005005*; NM_005125; NM_007103; *NM_024407*
electron transporter activity	20	295	4.06×10^{-3}	2.20×10^{-1}	*AF258341*; AK002110; AK056467; NM_000302; NM_000689; *NM_000903*; NM_002085; NM_002134; *NM_002495*; NM_002631; NM_004551; NM_004718; NM_005002; *NM_005005*; NM_006440; NM_007103; NM_015959; *NM_016593*; *NM_024407*; NM_030810

b

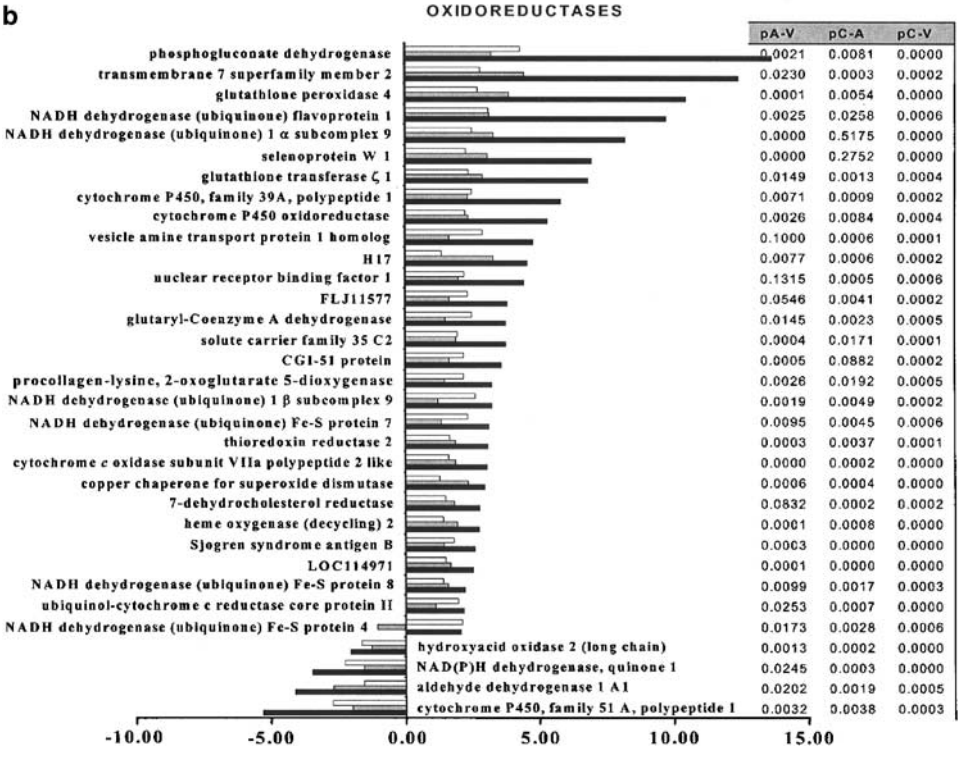

expressed between MCF-7 OPNc and MCF-7 vector according to normalized individual array ratios. The groups of genes affected by osteopontin-c (as compared to vector) include oxidoreductases and ion transporters according to EASE (Expression Analysis Systematic Explorer) analysis (Figure 5a, Supplement 1). Real-time PCR validation of these results confirmed the differential expression of glutathione peroxidase 4 (ΔC_T values compared to 18s RNA: MCF-7 vector – 3.54, MCF-7 OPNa – 5.27, MCF-7 OPNc – 7.63) and NADH dehydrogenase (ubiquinone) flavoprotein 1 (ΔC_T values: MCF-7 vector – 0.18, MCF-7 OPNa – 1.37, MCF-7 OPNc – 2.14). For pyruvate dehydrogenase (lipoamide) α1, a gene not identified as differentially expressed in the microarrays, the real-time PCR confirmed comparable expression levels among the groups (ΔC_T values: MCF-7 vector – 9.39, MCF-7 OPNa – 10.3, MCF-7 OPNc – 8.82). A comparison of the changes in expression of individual genes within the oxidoreductase group indicated that the changes for osteopontin-c versus -a were similar, but less extensive than for osteopontin-c versus vector (Figure 5B). This is not a dosage effect, because the amount of osteopontin secreted by MCF-7 OPNa was higher than the amount secreted by MCF-7 OPNc, as judged by Western blotting at the beginning of the soft agar experiment (data not shown).

Discussion

We have found that alternative splicing is one mechanism, by which cancer cells alter the structure and function of osteopontin, leading to increased anchorage independence. The functional implications of splicing of the small exon 4 (27 amino acids), which translates to a domain far N-terminal on the osteopontin protein, has been enigmatic. The multiple receptor binding sites for integrins and variant CD44 have been mapped to downstream regions (Weber *et al*., 2002) and the role of exon 4 was unknown. Osteopontin can form multimers that may participate in adhesion within mineralized tissue (Goldsmith *et al*., 2002) and there are functional differences between the soluble and the matrix-associated osteopontin (Adler *et al*., 2001; Rittling *et al*., 2002). As evidenced by the absence of connective tissue defects in the osteopontin knockout mice, the wide expression of the extracellular matrix protein osteopontin may not reflect important structural roles, but rather its availability for rapid release in stress responses, during which osteopontin is needed for immune stimulation and tissue remodeling. We have found that osteopontin-c strongly supports anchorage-independent growth. In contrast, osteopontin-a has an intermediate effect, possibly reflecting an equilibrium, in which a portion of the secreted product aggregates, with the remaining soluble portion supporting soft agar clone formation. Our data imply a paradigm, according to which the soluble form of osteopontin promotes metastasis, but the aggregated form does not. The exons 4 and 5 may play a critical role in osteopontin solubility.

Osteopontin has been known to exert strong effects on the redox status of various cells and to prevent programmed cell death in response to diverse stimuli (Hwang *et al*., 1994; Denhardt *et al*., 1995; Weber *et al*., 1999). The induction of various oxidoreductase genes by osteopontin, found in the microarray analysis, is consistent with these functions. Apoptosis frequently involves the generation of and signal transduction by free radicals (Weber *et al*., 1995). Anchorage independence in soft agar largely reflects resistance to a form of apoptosis referred to as anoikis. The induction of oxidoreductase genes by osteopontin may cause its antioxidant and antianoikis effects. These do not come into play during the growth of cells in culture dishes where oxidative stress or loss of anchorage are minimal, but they are prominent in semisolid medium. The role of the osteopontin-dependent upregulation of ion transporter genes in breast cancer remains to be clarified. It should be noted, however, that many of the genes in this group are also categorized as oxidoreductases (see Figure 5a). Osteopontin-c lacks a domain compared to the standard form of the molecule. This prevents it from aggregating and makes more soluble osteopontin available for receptor ligation. Consistently, most of the differences in gene expression detected by microarray are similar, but more extensive for osteopontin-c versus vector as compared to osteopontin-c versus -a or osteopontin-a versus vector. Of the 525 significantly differently expressed genes in the comparison of osteopontin-c versus vector, all but 20 changed in the same direction (induction or suppression) in the osteopontin-c versus -a hybridizations. Only a small number of genes may be uniquely induced by osteopontin-c. Further studies should clarify whether in addition to the loss of function, reflected in the lack of calcium-dependent aggregation and cell adhesion, osteopontin-c gains new functions, possibly through the ligation of a novel receptor.

It may be important to note that it is not unexpected for tumors to express multiple variant transcripts of metastasis-associated genes. Similar observations have been made for the homing receptor CD44. Tumors may express up to nine distinct spliced forms of this gene (Matsumura and Tarin, 1992). Only certain CD44 splice variants support metastasis (Gunthert *et al*., 1991), while the standard form acts as an inhibitor of dissemination (Tanabe *et al*., 1995). By inference, it is possible that full-length osteopontin tends to immobilize cells, while the spliced osteopontin variants may be critical to breast cancer metastasis. This is supported by our observation of aggregation of osteopontin-a, resulting in enhanced cell adhesion, at physiologic calcium concentrations. Exon 4 appears to be necessary for this function, because osteopontin-c remains soluble.

Alternative splicing of osteopontin is not known to occur in mice. By RT–PCR, we have not detected more than one message in various murine tissues (unpublished results). Overexpression of full-length osteopontin has induced invasive behavior in mouse tumor models. There are two possible reasons for this. The unphysiologically high level of overexpression

typically achieved by transfection may generate sufficient levels of nonaggregated osteopontin to facilitate cell migration. Alternatively, the apparent absence of osteopontin splicing in mice, typically used as an *in vivo* model for dissemination, may render them susceptible to full-length osteopontin. Owing to the restrictions in structural diversity of osteopontin, mouse models may have limitations for investigating osteopontin in cancer.

Materials and methods

Cell lines and reagents

MCF-7 cells, were grown in α-MEM with insulin and 10% fetal bovine serum (FBS). MDA-MB-435 cells were obtained from Dr Danny Welch and cultured as described (Seraj *et al*., 2000). The metastatic breast cancer cell line MDA-MB-231 (ATCC HTB-26) was grown in α-MEM with 10% FBS. ZR-75-1 (ATCC HTB-22) cells are derived from a ductal carcinoma, are tumorigenic but noninvasive. They were grown in RPMI with 10% FBS. 293T cells were used for transient transfections as previously described (He and Weber, 2003). The anti-osteopontin antibody was purchased from Assay Designs Inc. For application in the soft agar assay, a special order aliquot without azide was used.

DNA constructs and transfection

The constructs for expression of the human osteopontin splice variants were obtained by reverse transcription-PCR from the malignant breast tumor cell line MDA-MB-435. Total RNA was isolated by using RNeasy mini kit (Qiagen, Valencia, CA, USA) following the manufacturer's protocol. 1 μg of total RNA was used for cDNA synthesis with Super-script II reverse transcriptase (Gibco BRL, USA). The coding sequence of osteopontin was amplified with the primers 5′-CAA ACG CCG ACC AAG GGA AAA C-3′ and 5′-CTT CTT TCT CAG TTT ATT GGT-3′. The amplified product was TA cloned, excised with *Xho*1 and *Nhe*I, and was subcloned into the vector pCR3.1 (Invitrogen Carlsbad, CA, USA). Genes cloned into this vector are expressed under the control of the CMV promoter. Sequence fidelity and accurate reading frame were verified by DNA sequencing analysis. MCF-7 cells were transfected by the Fugene method and stable clones were selected in G418.

For the generation of GST-OPN fusion proteins, osteopontin cDNAs were amplified by PCR by exclusion of the signal peptide (1–17 amino acids) with the primers 5′-c ggg atc ccc ATA CCA GTT AAA CAG GCT GAT-3′ and 5′-gg ctc gag ATG TTC TCT TTC ATT TTG CTA-3′ using pCR3.1-OPNs as templates (the lower case letters show *BamH*I and *Xho*I sites and protective bases to facilitate cloning). The amplified fragments were subcloned into pGEX-5T vector and transformed into BL21 bacteria for making GST-OPN fusion proteins. Reading frames and sequence fidelity were confirmed by sequencing analysis.

Human breast cancer tissue

Specimens of human breast tumors, nontransformed surrounding tissue, as well as healthy breast tissue (obtained from reduction mammoplasties) were provided by the tissue procurement facility of the University of Cincinnati Medical Center.

RT–PCR

Total RNA was extracted from human tissues using Trizol^{R} (1 ml reagent/200 mg tissue), according to the manufacturer's protocol. 3 μg of total RNA was reverse transcribed by SuperScript II reverse Transcriptase (Invitrogen, Carlsbad, CA, USA). The osteopontin splice variants -a and -c were amplified with the primer pairs 5′-ATCTCCTAGCCCCACA GAAT-3′ (forward) and 5′-CATCAGACTGGTGAGAATCA TC-3′ (reverse) for osteopontin-a and 5′-CTGAGGAAAAG CAGAATG-3′ (forward) and 5′-AATGGAGTCCTGGCT GT-3′ (reverse) for osteopontin-c. The amplification of GAPDH with primers 5′-TGAAGGTCGGAGTCAACGGA TTTGGT-3′ (forward) and 5′-CATGTGGGCCATGAGGTC CACCAC-3′ (reverse) served as a control for equal loading and integrity of the cDNA. A 35 cycle touchdown PCR, with Taq DNA Polymerase and at 1.5 mM $MgCl_2$, was performed with five cycles at 59°C annealing temperature, five cycles at 55°C annealing temperature, and 25 cycles at 51°C annealing temperature. All PCR products were analysed by Tris-acetate EDTA agarose (2.5% w/v) gel electrophoresis. To confirm the specificity of the primer pairs for osteopontin-a and -c, we cloned and sequenced their PCR products from a representative tumor sample.

Immunoblot assay

For the analysis of secreted osteopontin, serum-free cell culture supernatant was collected from each transfectant. In all, 40 μl of supernatant per sample were electrophoresed on 10% SDS–polyacrylamide mini-gels with nonreducing sample buffer. For the analysis of intracellular osteopontin, the cells were lysed in RIPA buffer (50 mM Tris-HCl pH 7.5, 150 mM NaCl, 1% NP-40, 0.5% Na-deoxycholate, 0.1% sodium dodecyl sulfate). Cell lysates at equal amounts of protein (20 μg/lane) were electrophoresed on reducing 10% SDS–polyacrylamide gels. The separated proteins were transferred to PVDF membranes and probed with antibody O-17 (Assay Designs Inc.) to osteopontin.

Analysis of growth rates

For the investigation of cell growth rates, each cell line was plated at 5000 cells/well in 24-well plates. Daily, five wells per group were harvested by trypsinization and the cell numbers were determined in a Coulter™ Z-Series Counter. At each time point, the cell numbers from the five wells of the various groups of transfectants were analysed for statistically significant differences by the Wilcoxon–Mann–Whitney test and the *t*-test, accepting a probability of error of less than 5%.

Analysis of osteopontin aggregation

In all, 40 μl of supernatant from vector or OPN-a or OPN-c stable transfectants were incubated at 37°C for indicated time points in aggregation buffer (0.2 M NaCl, 0.05 M Tris-HCl, pH 7.6, 5 mM $CaCl_2$ final concentration) or at various Ca^{2+} concentrations for 16 h. The samples were resolved on reducing denaturing SDS/polyacrylamide gels and transferred to PVDF membranes followed by Western blotting.

Adhesion assay

In all, 96-well polystyrene plates were coated with the indicated amounts of GST-OPN forms or control fibronectin (50 μg/ml) in 100 μl/well at 4°C overnight. The wells were washed twice with cold PBS followed by blocking with 1% BSA for 1 h at 37°C. MCF-7 parental cells were used for assaying adhesion. The cells were trypsinized and treated with soybean trypsin inhibitor, then washed twice with PBS and resuspended in adhesion buffer (0.1% BSA, 1 mM sodium pyruvate, 2 mM

$MgCl_2$). Cells (2×10^4 cell/well) were added to the above 96-well plates and allowed to adhere at 37°C for 2 h. Nonadherent cells were removed by rinsing twice with PBS. Adherent cells were counted and photographed. For adhesion to aggregated osteopontin, GST or GST-OPN forms were added to 96-well plates in aggregation buffer (0.2 M NaCl, 0.05 M Tris-HCl, pH 7.6, 5 mM $CaCl_2$ final concentration) and incubated at 4°C overnight. All adhesion assays were performed with triplicate wells and were repeated at least three times.

Soft agar growth

In all, 1×10^5 cells per 60-mm dish were plated in triplicates with a top layer of 0.3% agar (BACTO Agar, Difco, Detroit, MI, USA) and a bottom layer of 0.5% agar (both in α-MEM). Every other day, 0.4 ml of medium was supplemented and the plates were examined microscopically for growth. After 1 week, photographs were taken at high and low magnification and the surface area of all clones in five fields was measured with the imaging software ImageJ (NIH) or Metamorph. The osteopontin expression levels on the day of plating were confirmed by Western blotting.

Microarray analysis

MCF-7 transfectants were plated in soft agar, following the confirmation of their osteopontin expression by Western blotting. After 7 days of soft agar growth, the clone sizes were measured and RNA was extracted with 2 ml TriReagent LS. Linear amplification was performed with the Amino Allyl Message Amp II kit from Ambion, and the samples were subjected to microarray analysis comparing MCF-7 OPNc, MCF-7 OPNa, and MCF-7 vector. For each comparison, several hybridizations (four for OPNc versus OPNa and two each for OPNa versus vector and OPNc versus vector) were performed with RNA from distinct soft agar plates and dye-flip of the fluorescent labels. The microarray experiment was carried out as described (Hosack *et al*., 2003; Karyala *et al*., 2003; Guo *et al*., 2004) (see also http://microarray.uc.edu). The human 70-mer oligonucleotide library version 2.0 (21 329 optimized oligos) (Qiagen, Alameda, CA, USA) were printed on aminosilane-coated slides (Cel Associates Inc., Pearland, TX, USA). Fluorescence-labeled cDNAs (Cy3 and Cy5; Amersham, Piscataway, NJ, USA) for hybridization were synthesized from linearly amplified total RNA using an indirect amino allyl labeling method via an oligo(dT)-primed, reverse transcriptase reaction. The data representing background-subtracted spot intensities were analysed after log transformation and data centering.

Statistical significance of differential expression was assessed according to *P*-values, and adjusting for multiple hypotheses testing by calculating false discovery rates (FDR) (Sartor *et al*., 2004; Benjamini and Hochberg, 1995). Estimates of fold-change were calculated, and the cutoff used for significance was a fold change of >2, an intensity of >100, and an FDR <0.05. Significantly changed transcripts were tested against functional assignments, to determine which gene categories were enriched with differentially expressed genes. This was performed with Expression Analysis Systematic Explorer (EASE), using the gene categories of the Molecular Function and Biological Process branches of the Gene Ontology database (Hosack *et al*., 2003). Gene Ontology is a multi-organism, controlled vocabulary database containing three separate ontologies: biological process, molecular function, and cellular component. It is commonly used for assessing the results of microarray analyses. Fisher's Exact Probability, using the Benjamini FDR adjustment, was calculated for each gene category (Reiner *et al*., 2003).

The microarray results were validated by real-time PCR, which was conducted using a Cepheid Smart Cycler and a SYBR Green detection format. Oligo-dT primed first strand cDNA was synthesized using Invitrogen SuperScript according to the manufacturer's protocol. The PCR reaction contained $0.5 \times$ SYBR Green (Roche Diagnostics), $MgCl_2$ and primer concentration were optimized for each gene. A 40 cycles PCR protocol consisted of 94°C melting for 15 s, specific annealing for 30 s, and 20 s extension at 72°C. Melt curves yielded a single peak in all cases with no primer dimers. A no-template control was included in all reactions. The levels of 18S rRNA were used to normalize for equal amounts of RNA.

Acknowledgements

This study was supported by National Institutes of Health research Grant CA76176 and Department of Defense breast cancer Grant DAMD17-02-0510 to GFW. The collection of tumor specimens was supported in part by USPHS Grant #M01 RR 08084 from the General Clinical Research Centers Program, National Center for Research Resources, NIH. Dr Danny Welch, Birmingham, AL, generously provided the MDA-MB-435 cells.

References

Adler B, Ashkar S, Cantor H, Weber GF. (2001). *Cell Immunol* **210**: 30–40.
Ashkar S, Weber GF, Panoutsakopoulou V, Sanchirico ME, Janssen M, Zawaideh S *et al*. (2000). *Science* **287**: 860–864.
Barraclough R, Chen HJ, Davies BR, Davies MP, Ke Y, Lloyd BH *et al*. (1998). *Biochem Soc Symp* **63**: 273–294.
Bayless KJ, Meininger GA, Scholtz JM, Davis GE. (1998). *J Cell Sci* **111**: 1165–1174.
Behrend EI, Chambers AF, Wilson SM, Denhardt DT. (1993). *J Biol Chem* **268**: 11172–11175.
Benjamini Y, Hochberg Y. (1995). *J Roy Stat Soc B* **57**: 289–399.
Chackalaparampil I, Banerjee D, Poirier Y, Mukherjee BB. (1985). *J Virol* **53**: 841–850.
Chen H, Ke Y, Oates AJ, Barraclough R, Rudland PS. (1997). *Oncogene* **14**: 1581–1588.
Chen PW, Geer DC, Podack ER, Ksander BR. (1996). *Ann NY Acad Sci* **795**: 325–327.
Crawford HC, Matrisian LM, Liaw L. (1998). *Cancer Res* **58**: 5206–5215.
Denhardt DT, Lopez CA, Rollo EE, Hwang SM, An XR, Walther SE. (1995). *Ann NY Acad Sci* **760**: 127–142.
El-Tanani M, Barraclough R, Wilkinson MC, Rudland PS. (2001a). *Cancer Res* **61**: 5619–5629.
El-Tanani M, Barraclough R, Wilkinson MC, Rudland PS. (2001b). *Oncogene* **20**: 1793–1797.
Goldsmith HL, Labrosse JM, McIntosh FA, Maenpaa PH, Kaartinen MT, McKee MD. (2002). *Ann Biomed Eng* **30**: 840–850.
Gunthert U, Hofmann M, Rudy W, Reber S, Zoller M, Haussmann I *et al*. (1991). *Cell* **65**: 13–24.
Guo J, Sartor M, Karyala S, Medvedovic M, Kann S, Puga A *et al*. (2004). *Toxicol Appl Pharmacol* **194**: 79–89.
He B, Weber GF. (2003). *Eur J Biochem* **270**: 2174–2185.
Hosack DA, Dennis Jr G, Sherman BT, Lane HC, Lempicki RA. (2003). *Genome Biol* **4**: R70.

Hwang SM, Lopez CA, Heck DE, Gardner CR, Laskin DL, Laskin JD *et al*. (1994). *J Biol Chem* **269**: 711–715.
Kasugai S, Zhang Q, Overall CM, Wrana JL, Butler WT, Sodek J. (1991). *Bone Miner* **13**: 235–250.
Karyala S, Guo J, Sartor M, Medvedovic M, Kann S, Puga A *et al*. (2003). *Cardiovasc Toxicol* **4**: 47–73.
Kiefer MC, Bauer DM, Barr PJ. (1989). *Nucl Acids Res* **17**: 3306.
Kon S, Maeda M, Segawa T, Hagiwara Y, Horikoshi Y, Chikuma S *et al*. (2000). *J Cell Biochem* **77**: 487–498.
Matsumura Y, Tarin D. (1992). *Lancet* **340**: 1053–1058.
Oates AJ, Barraclough R, Rudland PS. (1996). *Oncogene* **13**: 97–104.
O'Regan AW, Hayden JM, Berman JS. (2000). *J Leukoc Biol* **68**: 495–502.
Reiner A, Yekutieli D, Benjamini Y. (2003). *Bioinformatics* **19**: 368–375.
Rittling SR, Chen Y, Feng F, Wu Y. (2002). *J Biol Chem* **277**: 9175–9182.
Rittling SR, Feng F. (1998). *Biochem Biophys Res Commun* **250**: 287–292.
Rudland PS, Platt-Higgins A, El-Tanani M, De Silva Rudland S, Barraclough R, Winstanley JH, Howitt R, West CR. (2002). *Cancer Res* **62**: 3417–3427.
Saitoh Y, Kuratsu J, Takeshima H, Yamamoto S, Ushio Y. (1995). *Lab Invest* **72**: 55–63.
Sartor M, Schwanekamp J, Halbleib D, Mohamed I, Karyala S, Medvedovic M *et al*. (2004). *Biotechniques* **36**: 790–796.
Seraj MJ, Samant RS, Verderame MF, Welch DR. (2000). *Cancer Res* **60**: 2764–2769.
Singhal H, Bautista DS, Tonkin KS, O'Malley FP, Tuck AB, Chambers AF *et al*. (1997). *Clin Cancer Res* **3**: 605–611.
Sung V, Gilles C, Murray A, Clarke R, Aaron AD, Azumi N *et al*. (1998). *Exp Cell Res* **241**: 273–284.
Tanabe KK, Stamenkovic I, Cutler M, Takahashi K. (1995). *Ann Surg* **222**: 493–501.
Tuck AB, Arsenault DM, O'Malley FP, Hota C, Ling MC, Wilson SM *et al*. (1999). *Oncogene* **18**: 4237–4246.
Urquidi V, Sloan D, Kawai K, Agarwal D, Woodman AC, Tarin D *et al*. (2002). *Clin Cancer Res* **8**: 61–74.
Weber GF, Adler B, Ashkar S. (1999). *Inflammatory Cells and Mediators in CNS Diseases* In: Ruffolo Jr RR, Feuerstein GZ, Hunter AJ, Poste G, Metcalf BW (eds). Harwood Academic Publishers: Amsterdam, pp. 97–112.
Weber GF, Abromson-Leeman S, Cantor H. (1995). *Immunity* **2**: 363–372.
Weber GF, Ashkar S. (2000a). *J Mol Med* **78**: 404–408.
Weber GF, Ashkar S. (2000b). *Brain Res Bull* **53**: 421–424.
Weber GF, Ashkar S, Glimcher MJ, Cantor H. (1996). *Science* **271**: 509–512.
Weber GF, Zawaideh S, Kumar VA, Glimcher MJ, Cantor H, Ashkar S. (2002). *J Leukoc Biol* **72**: 752–761.
Yokosaki Y, Matsuura N, Sasaki T, Murakami I, Schneider H, Higashiyama S *et al*. (1999). *J Biol Chem* **274**: 36328–36334.
Young MF, Kerr JM, Termine JD, Wewer UM, Wang MG, McBride OW *et al*. (1990). *Genomics* **7**: 491–502.
Zhang G, He B, Weber GF. (2003). *Mol Cell Biol* **23**: 6507–6519.
Zitvogel L, Couderc B, Mayordomo JI, Robbins PD, Lotze MT, Storkus WJ. (1996). *Ann NY Acad Sci* **795**: 284–293.

Supplementary Information accompanies the paper on Oncogene website (http://www.nature.com/onc)